Addis Ababa University

Addis Ababa Institute of Technology (AAiT)

African Railway Center of Excellence

A Master's Thesis On:

Numerical Analysis of Wear Behavior of Rail Material: A case study on Addis Ababa Light Rail Transit

Submitted in Partial Fulfillment of the

Requirements for the Degree of Master of Science in Railway

Engineering (Rolling Stock)

By: Lucky Ugochukwu Adoh

Advisor: Dr. Samuel Tesfaye

Co-Advisor:

Mr Tollosa

Addis Ababa, Ethiopia

July 2020

Numerical Analysis of Wear Behavior of Rail Material: A case study on Addis Ababa Light Rail Transit

Approval

The undersigned have examined the thesis entitled '**Numerical Analysis of Wear Behavior of Rail Material: A case study on Addis Ababa Light Rail Transit'** presented by Lucky Ugochukwu Adoh, a candidate for the degree of Master of Science in Railway Engineering (Rolling Stock) and hereby certify that it is worthy of acceptance. Submitted by

Lucky Ugochukwu Adoh	……	…….
Student	Sign	Date

Approved by:

Dr. Samuel Tesfaye	…….	……
Advisor	Sign	Date

…….	…….	……
Internal Examiner	Sign	Date

…….	……..	……..
External Examiner	Sign	Date

…….	……..	……..
Chairperson	Sign	Date

Numerical Analysis of Wear Behavior of Rail Material: A case study on Addis Ababa Light Rail Transit

Undertaking

I certify that research work titled "**Numerical Analysis of Wear Behavior of Rail Material: A case study on Addis Ababa Light Rail Transit** " is my own work. The work has not been presented elsewhere for assessment. Where material has been used from other sources it has been properly acknowledged/referred.

Lucky Ugochukwu Adoh

…….

Numerical Analysis of Wear Behavior of Rail Material: A case study on Addis Ababa Light Rail Transit

Abstract

The railway track is one of the most important element of a railway system. During passage of trains, the rails are subjected to contact load that comes from the wheels of the train. The railway track often fail in service due to wear caused by contact fatigue and other wear damage mechanisms. It is worthy to note that no matter how perfect the rail vehicle is designed to be, if the rails is not in good conditions with a minimal fatigue and wear damage, this will definitely affect the life span of the railway infrastructure and railway vehicle. The aim of this research is to investigate the wear behavior of a rail material under the effects of variable vehicle loads, coefficient of friction and running speed of the train. In this study wear parameters (wear rate, and wear volume) are analyzed by numerical modeling using SIMPACK. The wear behavior of Addis Ababa light rail transit rails was studied (straight track section of the north-south line). The effects of coefficient of friction, wheel load and vehicle speed was investigated. From the study, it was found that the highest specific wear rate for the overload capacity of the train is 1.271234×10^{-4} mm ^{3}/Nm while the lowest specific wear rate is 0.000453×10^{-4} mm ^{3}/Nm. The highest specific wear rate occurred at the maximum operating speed of the train (70 Km/hr) while the lowest specific wear rate occurred at a speed of 20 Km/h. This shows that as the running speed of the train increases, the specific wear rate increases. So in other to increase the wear life of the rails in Addis Ababa light rail transit, it is imperative to use medium friction coefficient (0.25 to 0.35) values and operate the train between the speed ranges of 20 to 40 Km/hr.

Keywords: *Addis Ababa light rail transit rails, loading conditions, friction, running speed, sliding distance, wear parameters*

Dedication

I would love to dedicate this research work to my mother, Mrs Christiana Adoh, who stood by me throughout the duration of my bachelor's and master's study. God bless, keep and increase you my ever precious mother.

Acknowledgement

My profound gratitude goes to almighty God, who is my helper, who has always being my shield against all evil plans, and who has always strengthened me to conquer and has kept me till this day.

My sincere gratitude to my highly esteem thesis supervisor, Dr. Samuel Tesfaye for your, scholarly, friendly and brotherly advise and correction during the period of carrying out this research. He is the map and compass of this project, who told me what to do, when to do, and how to do it. Thank you sir for your time and understanding. I could not have gotten a better adviser than you. May the good God grant you your heart desires.

I also appreciate all those who always pray for me even though I do not know you.

I also appreciate all my friends, fans and well-wishers. God bless you

I also appreciate the Ethiopia railway corporation for their support with giving out data for this research.

I also appreciate the World bank through the African Railway Center of excellence for giving me this scholarship.

Table of Contents

Nomenclature

AALRT – Addis Ababa Light rail transit

FEM- finite element methods

FEA- Finite element analysis

COF – Coefficient of friction

SWR - Specific wear rate

List of figures

List of Tables

Numerical Analysis of Wear Behavior of Rail Material: A case study on Addis Ababa Light Rail Transit

Chapter One

1.0. Introduction

1.1 Background

Since the first iron track was developed in 1738 [1], railways have been playing an important role in public transportation. In Ethiopia, The first rail transportation (train service) began on July 22, 1901, and operated between Djibouti and Douala, the first station on the Ethiopian side of the frontier at kilometer 106, a journey of 51/2 hours [2] . By 1915 the line reached Akaki, only 23 kilometers from the capital city, and two years later came all the way to Addis Ababa itself [2] . This marked the official commercial opening of the 784 km long railway although the Station of Addis Ababa was not inaugurated until 3 December 1929.

In September 2015, Ethiopian introduced the first light rail transits system at Addis Ababa city (ALART)[3]. It was the first in Sub Saharan Africa which joined the few African capitals with urban train facilities. The $475 Million worth environmental friendly light railway transport started service on September 20, 2015 charging the lowest fare of 2 Birr per 4km [4]–[6].

Thus, this study focuses on Addis Ababa light rail transit real conditions. The railway transport system is one of the most crucial transport systems in the world with mass transport, very high speed, safety and durability. Nowadays, there is a high demand for railway transportation systems in the world including in Ethiopia for a short and long distance transport of passengers and goods. The new rail network in Ethiopia and the railway track must show the necessity of an efficient management of railway systems. The design must aim toward reducing costs and increasing safety, as well as reliability of the railway systems. The wheel/rail interface is one of the most crucial points that must be checked to determine the performance of a train and consider its safety [7].

Railway transport during the last years has increased in speed, security and comfort. In comparison to automobiles, railway transport is a more secure and less environment damaging means of transportation. In order to keep up the competiveness of railroad transportation, increasing requirements on the speed of passenger and freight trains, on the axle load of the trains as well as the comfort of the passengers have to be met. Further pressure on the development arises from the demand of decreasing the costs of both new trains and new rail tracks as well as the maintenance costs. Thus a large number of investigations have focused an optimization of trains, rail tracks and the rail/wheel system. For instance, optimizing the rail top profile. The mechanisms of material changes at the rail-wheel interface also have received considerable attention. But, so far the

structure changes that occur in the rail and the wheel material during service still have not been completely solved and clarified. In service the surface of the rail track as well as the surface of the wheel sets are subject to strong changes due to their long time sustaining load and wear.

The damages that affect the mechanisms of wear are some of the concerns for the life prediction for a railway rails. Wear causes abrupt fractures in the railhead and wheel tread. These failures may cause damage to rails because of the stress caused by the contact force. This study presents the numerical investigation of wear damage due to cyclic axle load on the rail and wear life for the light rail transit (LRT) in Addis Ababa, Ethiopia.

1.1.1 Railway Track

The railway infrastructure is a tracks with all the appropriate facilities plants and other devices, which are in function at the railway traffic [8]. In railway system, the main function of the track are guiding the train, carrying the loads and distribute the load to a larger area. For instant, a normal load of 10 tones, would create a few square meters [9]. The structure of the track is shown in figure 1 which includes some components such as rails fastening, sleeper, ballast and subgrade. The details of each component are as follows

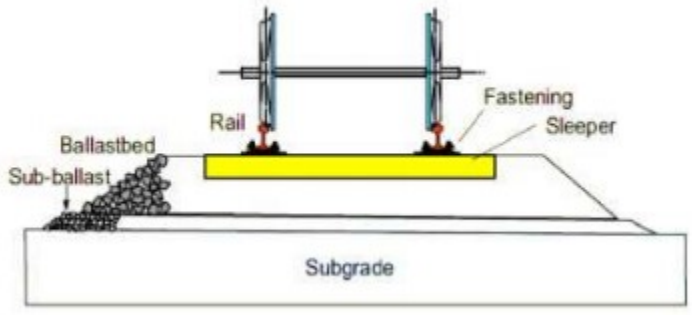

Fig. 1.1. Cross section of the railway track [9]

In order to increase the speed of trains, axles loads of trains, traction and density of traffic requires improved quality of rails [10]. Rails which is an important part of railway infrastructure have exact level of quality.

1.1.2. Rail terminologies and Profile

Some of the terminologies concerned with the railway track are discussed as below [11];

- Field Corner Region: top corner on the field side of the rail
- Fishing Surface: the region at the bottom of the rail head, which makes contact with

fish plates

- Rail Head: The region of the rail that is above the extensions of the fishing surfaces to the rail Centre line
- Running Surface: zone on top of the rail head, which makes contact with wheel tread.
- Rail Web - the region of the rail that is between the rail head and the rail foot
- Top of Rail Foot : The region on top of the rail foot, which makes contact
- Gauge Corner Region: top corner on the gauge side of the rail, which makes contact with the wheel throat region.
- Rail Foot: the region of the rail that is below the extensions of the top of foot surfaces to the rail Centre line.
- Bottom of Rail Foot : The region on the bottom of the rail foot, which makes contact with sleeper plates or rail pads

1.1.3. Rail wear

The gradual removal of material from the surface of the rail which can lead to separation or cutting of rail due to friction and abnormal heavy load is known as rail wear**.** There are three types of wears of rail [12].

1. Head of rail wear

The metal from the top surface of rail flows and forms projections which are known as burns (fig.5). The causes of such types of wear are:

- Rails are worn out on top due to abrasion of the rolling wheels over them.
- The heavy wheel loads are concentrated on very small areas.
- Impact of heavy loads
- Corrosion of metal of rails
- Due to slipping action of wheels during starting and when brakes are applied to the moving trains, the metal of top of rail burns.

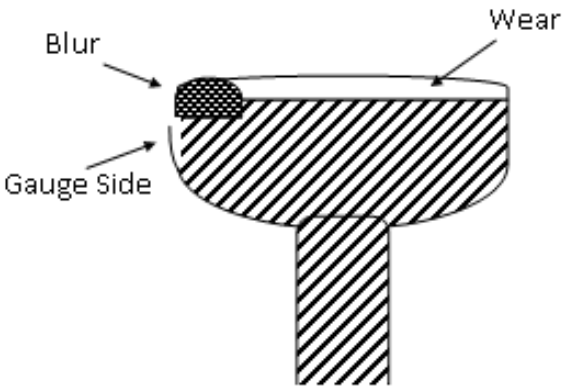

Fig. 1.2. Wear on Rail top surface[12]

2. Wear at the End of rails

This wear of rails takes place at the ends of rails and is found to be very much greater than the wear at the top of rails. At the expansion gap, the wheels of the vehicle have to take a jump and during this jump, they impart a blow is the ends of the rails. This blow is the main cause of wear of rails at ends. Due to successive blows, the ends of the rails are battered.

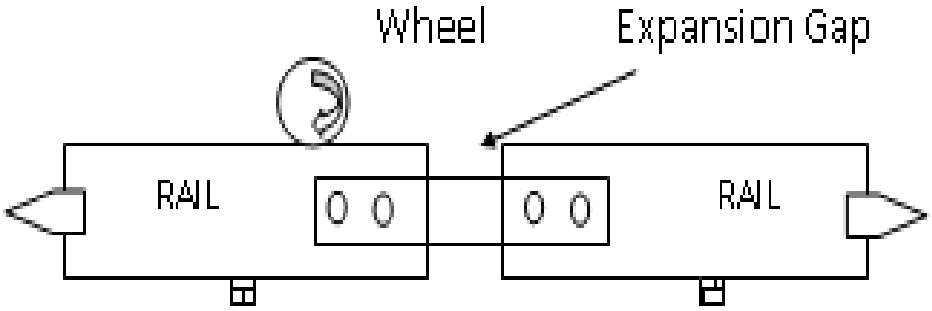

Fig. 1.3. Wear of Rails at Ends [12]

3. Wear at the side of head of rails

This is the most destructive type of wear and occurs on the rails on curves. The various causes of side wear of rails are:

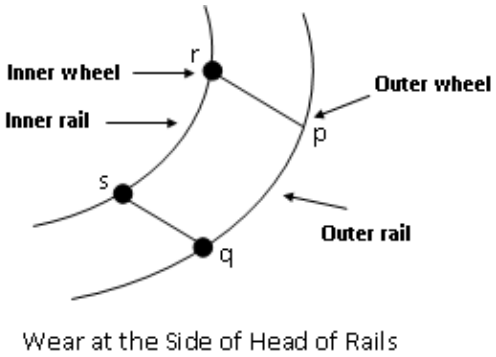

Fig. 1.4. Wear at the side of Rail Head [12]

- Due to centrifugal force along the curvature, the grinding action of wheel flanges on the inner side of the head of the rails is caused.
- The vehicles do not bend to the shape of the curvature while moving over a curve. This results into the biting of the inner side of the head of outer rail by wheel flanges.
- The wear on the inner side of the head of inner rail is mainly due to the slipping action of wheel on curve. Outer wheels have to cover a longer distance than inner wheel. But due to rigid connection between two wheels, they cover the same distance and hence then inner wheel slips over the inner rail, resulting in the wear of inner side of head of inner rail.

1.1.4. Stresses in rails

There are four kind of stress that occur in railway track; contact, bending, thermal, and residual stresses [11]. They are described below;

1. **Contact stress**

Contact stress is the stress developed due to relative motion between two surfaces in contact. Usually, one of the surface is hard and the other one is soft. For the case of wheel and rail contact, the rail surface is hard while the wheel surface is the soft.

2. **Bending Stresses**

Bending stress can occur in rails due to the following; the vertical loads applied to train wheel, which cause the rail to bend vertically between the sleeper supports which leads to tensile

longitudinal stresses in the rail foot, the applied lateral wheel loads which cause the rail head to move laterally relative to the foot which leads to tensile vertical stresses in the rail web, the vertical loads that are applied at some distance from the rail centre line, which leads to torsion of the rail, which can also cause additional tensile vertical stresses in the rail web.

3. Thermal Stresses

These stresses occur in long welded or continuously welded rails because of the longitudinal thermal expansion and contraction that occurs as the actual rail temperature increases above or reduces below the stress free temperature at which the rails are field welded. When the rail temperature is above the stress free condition, compressive longitudinal stresses are established. When the rail temperature is below the stress free condition, tensile longitudinal stresses are established, which influence the development of rail defects particularly in the transverse plane.

4. Residual Stresses

These stresses occur in railway track because of the manufacturing processes that are applied. In particular roller straightening and head hardening. These may include hot-rolling, roller-straightening and head-hardening. Then, in service, the running surfaces of rails are subjected to repeated rolling-contact stresses through contact with the train wheels. These stresses are usually high and they can cause plastic deformation around the contact surface and modify the stress field near the running line and internally in the railhead

1.1.5. Rail corrugation

Rail corrugations are cyclic (wave-like), generally vertical, irregularities on the running surface of the rails. Corrugations are of two main types; Short pitch (30mm to 90mm in wavelength,) and the long pitch (closed to 300mm in wavelength) [11].Irregularities on wheels and rails give rise to noise, ground-borne vibration and more general dynamic loading, which increases damage of components of both vehicle and track. Both wheels and rails are prone to develop quasi-sinusoidal irregularities, which are known as corrugation when their wavelength is less than about a meter [13].

Fig. 1.5. Railway Rail corrugation [14]

1.1.5.1. Causes of Rail corrugation

Significant rail corrugation can decrease the service life of tracks and make the replacement of the affected track necessary. Rail corrugation is caused by the friction between the rail and the train wheels tangentially, vertically, and axially [15]. Wear corrugation is a result of friction on the lower rail, which comes in contact with the train wheel. Excessive corrugation can be identified by the wavelength found on the higher, or outer rail [15]. Rail corrugation may be limited or lessened with the use of heat treated or alloyed rails, as opposed to the traditional carbon composite rail. It is generally accepted that a few distinct causes lie behind different wavelengths of railroad corrugation (Grassie,2009)[13]. One study indicates that the specific short-wave railroad deformity is mainly caused by pinned-pinned resonance, in which the rail vibrates as a fixed beam, as if pinned between periodically placed sleepers.

1.1.6. Wheel Load on the rail

The loads on the wheel acting on the rail can be divided into three components; vertical, lateral and longitudinal loads. The vertical load results from the weight of the wheel and the car bodies. The lateral load is due to the movement of the wheel set on the rail, and is high on the curve track. The longitudinal load is the traction force which is generated by the rail vehicles. The magnitude of the forces acting between the wheel and the rail must be set to a limit by railway

company or organization. For instance, to avoid any initiation of surface damages on the rail surface such as crack or plastic deformation, the international unions of railways (UIC) sets the vertical wheel load to below 112.5 KN per wheel for static load, and from 160 KN to 200 KN per wheel for dynamic load depending on maximum speed of train. When a train running on a small radius curved track (less than 600 m), the force is set to a limit of 145 KN for the quasi-static vertical force and 60 KN for the quasi-static lateral force [16] . Likewise the forces at the contact patch also include normal and two tangential components (longitudinal component acting along the running direction, and lateral component acting in the plane normal to the running direction) [17] .

1.2. Problem Statement

Safety is a major public concern in our daily life. Annually, people have lost their lives due to railroad accident which is caused by faulty railway tracks. Conditions such as loading, running speed, friction and vibration can cause significant damage to the rail and wheels due to wear. Wear reduces the lifespan of the railway rails and increases maintenance cost and hence increases the operational cost of the railway infrastructure. The wear behavior of rails in Ethiopia has not been studied extensively, we only have the information has provided by the railway company. Thus, this study intends to investigate the wear behavior of railway rails by varying the vehicle load, coefficient of friction and speed in order to understand and predict the wear behavior of the rails.

1.2.1. Research questions

This study seeks to answer the following questions.

1. How loading conditions (empty, full and overload capacity) affect the performance of the rail?
2. How coefficient of friction affect the wear life of the rail?
3. How operating speed affect the wear life of the rail?
4. What is the wear rate of AALRT rail?

1.3. Objectives of the study

1.3.1 General Objective

The main objective of the study is to investigate the wear behavior of a railway rail. The specific objectives are listed as;

1.3.2. Specfic objective

1. Numerical Modelling of the AALRT railway rail using SIMPACK.
2. Analyze the effects of coefficient of friction, wheel load and operating speed on wear parameters of the railway rail.

1.4. Significance of the study

This research has a great role to play for future analysis and production of railway rails by the Ethiopian Railway Corporation. Some of the benefit of this study if implemented can help in;

1. Reducing the wear failure of railway rail.
2. Improving the wear life of the AALRT railway rail.

1.5. Research Methodology

Fig. 1.6 shows outline or work flow of the methodology taken in this research.

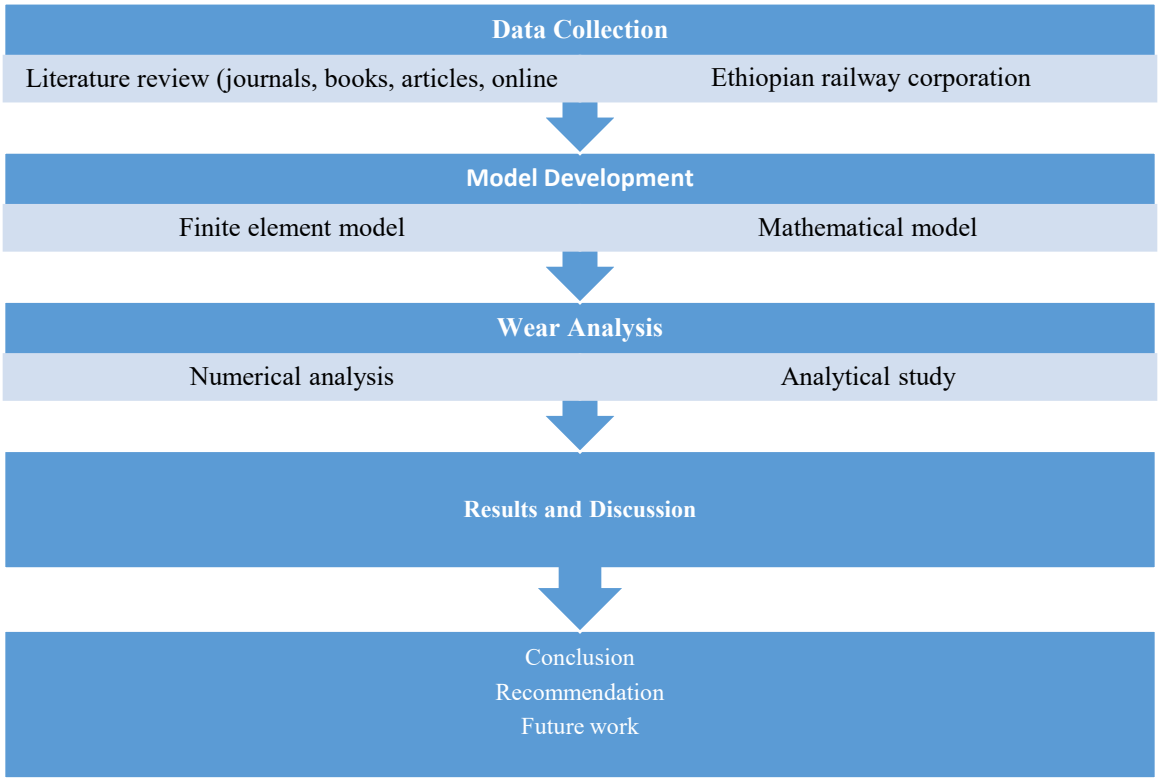

Fig. 1.6. Research outline

1.6. Scope of the study

This research limited to the wear analysis of rails and does not include the railway track components like sleepers, ballast etc. Nonlinear behavior of which some components could

experience is not dealt with and linear and isotropic material models are used for the entire analysis in the case of the finite element analysis. In the static analysis (FEM) of the railway track, damping properties of the structures is not considered. This research does not cover fatigue and wear analysis of the rail joints. This study is to improve the wear rate of AALRT railway rails.

1.7. Thesis Outline

This thesis contains four chapters. The content of each chapter is briefly described below; Chapter one contains general information about the research conducted. Initially, the basis behind the research are discussed and presented. This is followed by the general and specific objectives of the research. After that, the scope and the limitations of the research are pointed out. Finally, the thesis structure is presented by summarizing all of the chapters. Chapter two reviews published literatures relevant to the thesis topic. The cause and the methods for analysis of wear behavior of rails. Also the analysis and prediction of wear life of the rail is seen. Numerical/Analytical methods and conditions are described in chapter three. Chapter three describes the material type used for the analysis and conditions of operation This chapter also describes the dimensions of the specimens. Additionally, the FEA by SIMPACK software is modeled.

Chapter four describes the results found by SIMPACK for wheel/rail and the specimen analyzed by this software. The main findings of the study are also summarized in chapter 5 along with recommendations for application and also improvement or/and related studies are suggested for future work.

Chapter two

2.0. Literature Review

2.1 Introduction

This section comprises of a review of different studies on the wear of railway rails. Researches in wheel/rail interaction are essential in maximizing the efficiency of the rail vehicle and capacity utilization of the rail infrastructure. Some of the recent research field in wheel/rail tribology include but not limited to; contact mechanics involving forces and relative motion between the wheel-rail rolling contact, rolling contact fatigue in crack formation and crack growth in the material close to, or at the wheel-rail interface, fracture mechanics which deals with the strength of cracked components and can be employed to predict final fracture of a rail, research on materials which concerns both the refinement of existing materials and the development of new types of materials, study on tribology is necessary to understanding and optimizing the wheel-rail interface and research on railway which noise includes its generation, radiation and propagation to the surroundings and to the passengers cabin.

One of the importance of studying rail wear is to improve the safety of the railway infrastructure. Some authors [18], [19] has done work regarding safety of railway infrastructure. While other researchers [15], [20], [29]–[31], [21]–[28] have studied on the wear of railway rails.

Dirks [24] opined that the location of the highest wear on rails depends on whether the rail is located in a curve or on straight track. Two examples of what worn rails can look like are shown in Figure 3.2. In a curve, the rail is exposed to higher creep forces and creepages and will show more wear. Since the wheel-rail contact on the outer (high) rail in a curve is located at the gauge corner, the highest wear will take place here as well.

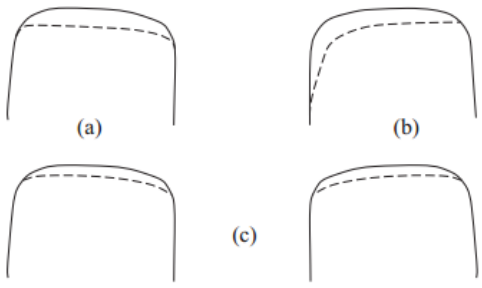

Fig. 2. 1. Worn rail profiles as dashed lines, (a) inner (low) rail in a curve, (b) outer (high) rail in a curve and (c) on straight track [24]

Majority of the wear on the railway rail is caused by the impact of the wheel load on the railway track. Railway rails are subjected to a range of loading conditions, from light to heavy rail vehicles and low to very high velocities as well as arctic to tropic environments [32]. The maintenance costs of rails and wheels are mainly influenced by wear and rolling contact fatigue (RCF) [24]. The two most important component of railway rail damage are damage caused by rolling contact fatigue and damage caused by wear mechanisms. It is worthy to note that, as wear of the rail increases, the fatigue life of the rail also reduces. The figure below shows the wear caused by scratches on the rail.

Fig. 2. 2. Scratches causing rail wear [33]

Franchima [34] studied about the potential causes of broken rail. He opined that faulty Rail, bolt hole stress cracks, wheel / engine burns and faulty weld are some of the causes of broken rail which has a negative effect on the railway rail. He opined that the metallurgy and manufacturing process of the rail are very vital to the longevity of the rail. If one or both are deficient, some form of irregularity can be introduced in the grain structure of the rail which can be a starting point for cracks. From splitting at the head (vertical or horizontal) to the web or foot of the rail, a crack can form at any point where the grain structure is irregular. He also gave several means of detecting a broken rail; visual examination, electrical continuity test and Nondestructive test (NDT). The visual examination involves a railway employee walking alongside the rail and visually examines the rail for irregularities and also the railway employee may use a test device that outputs data in real time. One of the short coming of this method is that it will not detect flaws beneath the rail surface. The electrical continuity test involves putting a low voltage through the rail to create a circuit. On one side is a power source, and on the other a relay. Once a fracture is detected on the

rail the relay will trip. This method can detect complete fractures on the rail but cannot detect any flaws that leave an electrical path around it. The Nondestructive testing involves ultrasonic and induction testing methods on rail lines to detect unseen flaws. The induction testing, a testing apparatus passes along the rail creating a very strong magnetic field in the railroad track and sensing any disturbances that may be caused by a defect. By introducing large amounts of low voltage current through the rail with two electrodes on either side of the sensing coil, the testing area is relatively small and accurate.

Fig. 2. 3. Broken rail [35]

2.2. Rolling contact fatigue

RCF is associated with plastic deformation under contact forces and a crack initiates (Figure 2.1) due to a unidirectional accumulation of strain that propagates downward under successive applications of compressive contact stresses. Factors affecting RCF are rail curve radius, wheel base, wheel diameter, axle load, primary yaw stiffness of suspension, rail-wheel profiles, traction, braking forces and wheel/rail material property. The stress concentration feature which causes initiation of RCF cracks is the contact between the wheel and the rail. Conditions under the contact patch are always severe and the yield stress of the rail steel is always exceeded, on at least a microscale, due to the surface roughness of the wheel and the rail. It follows that irreversible events take place at every passage of every wheel. The term ‘permanent way’ is a misnomer, because it is changing continuously. The irreversibility of each wheel passage, result in both a wear and a fatigue process and the resultant life of the rail is a competition between these two failure processes

[36]. The stresses generated under the contact are complex and governed by the detail of the wheel/rail geometry near the contact patch, the position of which is determined by, inter alia, curving behavior, vehicle suspension characteristics, and, of course, existing conditions of the wheel and rail. Both traction forces and radial curving forces increase shear stresses in the contact zone and hence the propensity to initiate cracks.

The mechanism of development of RCF cracks in rails is shown schematically in Fig. 2.4

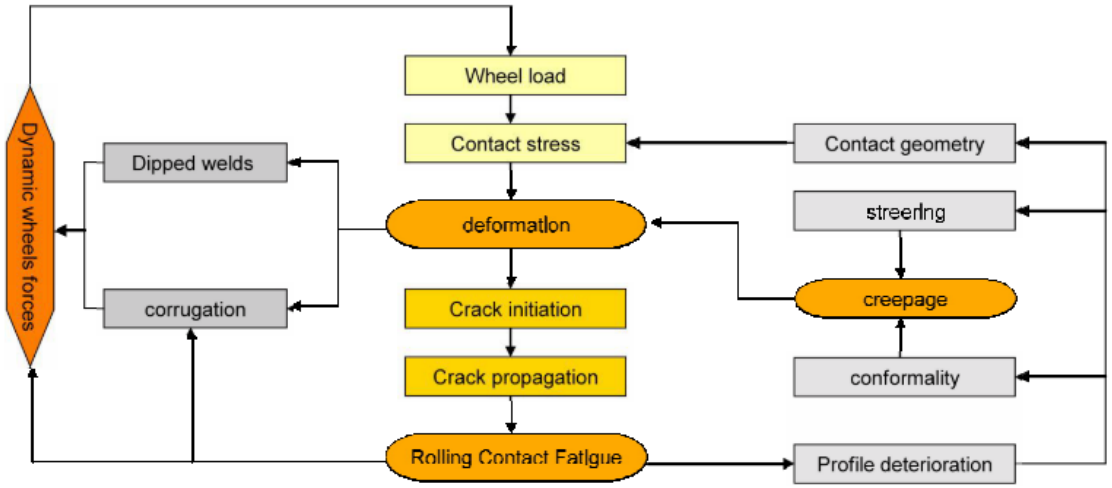

Fig. 2. 4. Stress Strain Vicious Cycle for RCF [37]

Jeong & Orringer [38] predicted surface crack growth in rail webs (Fig. 2.5) using FEM and elementary beam analysis. Both models were based on different assumptions but the calculated crack growth rate was found to be very slow in both cases allowing detection long before failure. Olofsson [39] have studied crack initiation and propagation with and without lubrication in two different rail steel grades (UIC900 A of UTS900N/mm2 and UIC1100 A steel of UTS 1100N/mm2) over two years in real rails with curve radii of 300mm and 600mm. Both materials seemed to be similarly sensitive to crack initiation but the 1100 grade rail was more sensitive to crack propagation and also more sensitive to head-checks, showing signs after 1 month of traffic as opposed to two years for the 900 grade. As expected, lubrication reduced the amount of profile change and also reduced the crack propagation rate, which was less expected. They explained this by the reduction of coefficient of friction, leading to lower tangential stresses in the contact zone between wheel and rail. Sensitivity to crack initiation on lubricated 1100 grade rail was still the same but the crack length and wear rate were reduced.

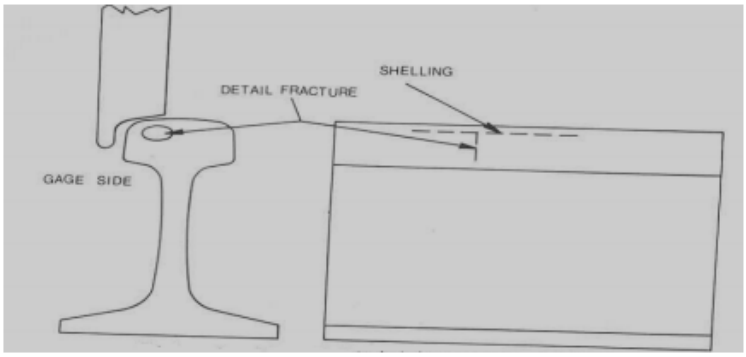

Fig. 2. 5. Schematic of wheel/rail contact showing shelling and detail fracture [38]

Akeel [40] studied damages on the rail head surface and wheel tread due to rolling contact fatigue. His paper analyses RCF damage initiation and stress distribution at the wheel/rail interface at different directions. A three-dimensional elastic frictional finite element model of the wheel/rail interaction is used to investigate the effect of the applied contact loading force at the straight, transition, and curved areas of the wheel tread and railhead surface. The interface exhibits small damage problems that are solved via the finite element method (FEM). The half space assumption of the Hertz method is avoided by FEM. The result indicates stress decreases at the straight area in the wheel-rail contact model compared with those at the transition and curved areas of the rail track. The effect of fatigue damage life initiation increases at the straight area but decreases at the transition and curved areas in the wheel/rail contact model and the maximum value of fatigue life prediction at the straight area.

Farris [41] found a reasonable correlation between calculated and experimental rates of shell crack growth, horizontal rail cracks located about 6-7mm below the surface of the rail. The shells are generally considered to be benign as they are not associated directly with rail failure, although they may grow out of the horizontal plane and cause vertical detail fractures that can lead to rail failure. Here, the leading edge of a short shell grows out of plane and initiates detail fracture in unidirectional train traffic. However, the trailing edge is branching up towards the surface and, when the train traffic is reversed, the leading edge becomes the trailing edge so a wavy crack path arises due to out of plane growth.

2.3. The Rail-Wheel Contact

As discussed earlier, majority of the wear on the railway rail is caused by the impact of the wheel load on the railway track. Sliding phenomena inside the contact patch, the normal force

transmitted, the friction coefficient, lubrication conditions, size and shape of the contact patch are some of the factors that causes wear on the rail. Worn profiles tend to be less stable and show lower performance levels when negotiating curved tracks, and this makes reducing the wear index a major factor in the design of railway vehicles [42].

The wear of materials has been characterized by weight loss and wear rate. However, Studies have found that wear coefficient is a more suitable factor [43].

Schilke [32] studied on the rail damages which are initiated and advanced by the rail wheel contact. He suggested that crack initiation is preceded by plastic deformation of the patch of the rail that is in contact with the wheel. There are normal loads caused by the axle loads and shear loads caused by traction, braking or flange contact. The normal loads cause slight to medium work hardening which, depending on the rail grade, can reach as deep as several millimeter [32]. The deformation caused by shear loads does not reach as deep as the normal load caused deformation Ekberg [20], but the shear load deformation leads to much higher strains in the material. The rail steel becomes heavily plastically deformed and the microstructure becomes aligned in the shear strain direction, Large amounts of material can be moved which can lead to the phenomenon of tongue lipping. This means that material on the flank of a rail flows downwards along the flank, where the flange contact of the wheel is most severe, to end up at a point just under the flange contact, creating a bulge of the rail profile that actually exceeds the original cross section of the rail as shown in Fig. 2.6.

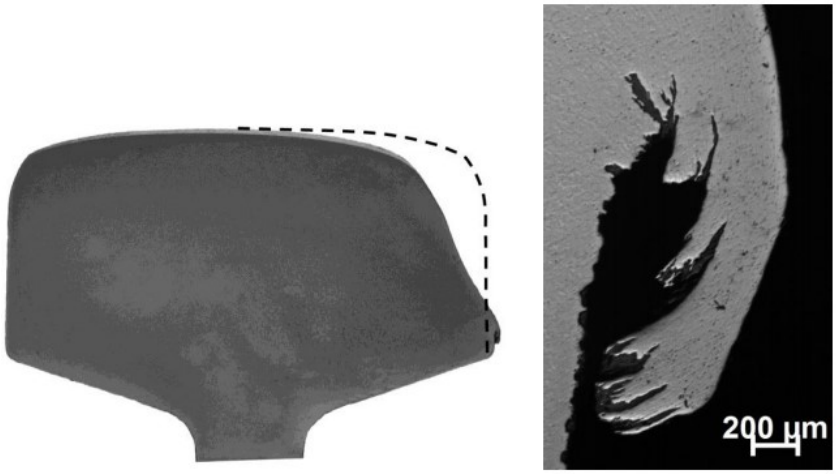

Fig. 2. 6. Wear of rail profile [32]

Dirk [24] suggested that the location of wear on a rail or wheel depends on where the contact position is. The amount of wear will be much less when the vehicle is running on straight track since the wheels are mainly rolling with very little sliding.

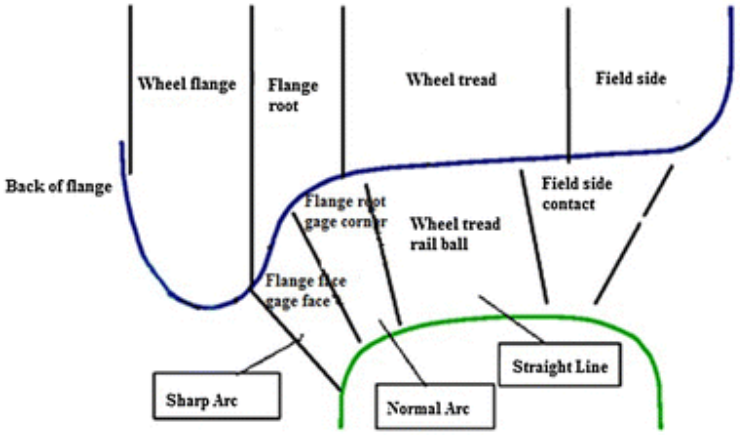

Fig. 2. 7. Contact points of the rail and wheel in a variety of paths [44]

2.4. Wear Mechanism

Wear resistance is considered as one of the most important characteristics of a rail steel. Wear is the loss or displacement of material from a contacting surface. Material loss may be in the form of debris. Material displacement may occur by transfer of material from one surface to another by adhesion or by local plastic deformation [25] . There are up to 35 different wear mechanisms that can occur between contacting bodies each of them producing different wear rates. The simplest classification of the different types of wear that produce different wear rates is mild wear and severe wear [27]. Mild wear results in a smooth surface that often is smoother than the original surface. On the other hand, severe wear results in a rough surface that often is rougher than the original surface [45]. Mild wear is a form of wear characterized by the removal of materials in very small fragments. Mild wear is favorable in many cases for the wear life of the contact as it causes a smooth run-in of the contacting surfaces. However, in some cases it has been observed that it worsens the contact condition and the mild wear can change the form of the contacting surfaces in an unfavorable way.

The main reason why wheel/rail wear is so important is safety against derailment. When the shape of the rail and wheel profiles is changed due to wear, a train could usually derail more easily [24].

Different wear mechanism and their interrelations [46] are shown in Fig. 13. Many wear mechanisms exist and there are several that are dominant in the wheel-rail contact [23], [24], [33]. Thermal wear processes are those directly associated with the increase in temperature caused by frictional heating in the contact. The principal type of wear process in this category is when a material melts or softens to such an extent that it can be displaced like a viscous fluid. Other mechanisms, such as adhesive wear, are also accelerated by a reduction in hardness. Other types are linked with thermal stresses that can cause thermal fatigue and cracking, which lead to loss of material.

Oxidative wear occurs under mild contact conditions, when the forces and sliding velocity are low. Under the influence of water and oxygen, oxides form on the surface and will eventually break away in the wheel-rail contact.

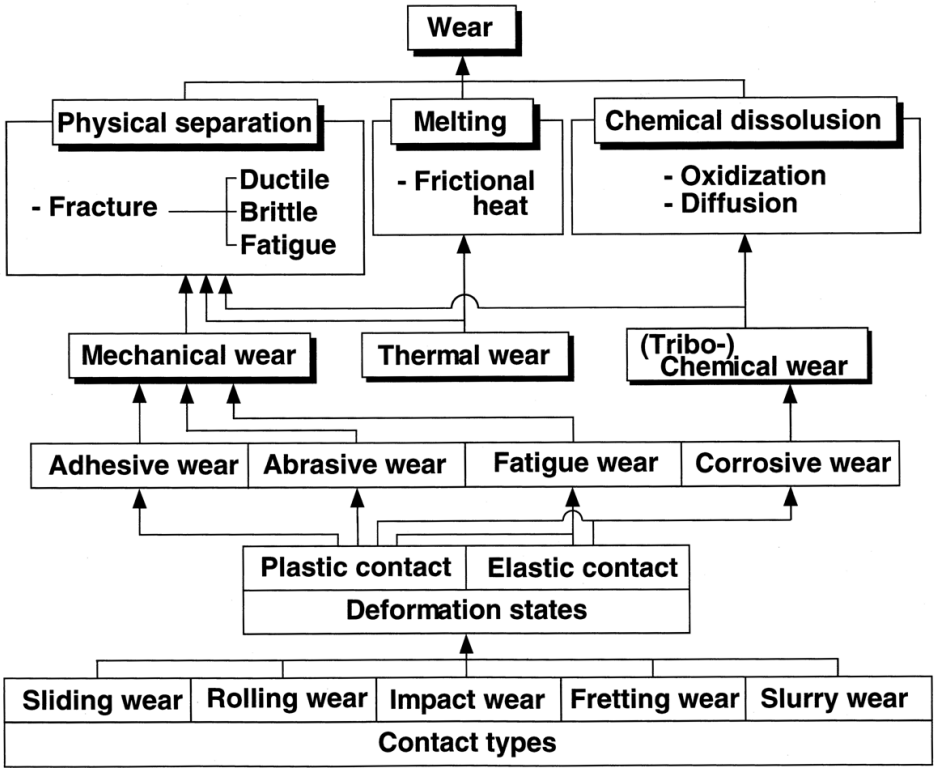

Fig. 2. 8. Wear mechanism and their interrelations [46]

Adhesive wear occurs when the adhesion forces in a sliding contact are high; shear takes place in the weakest material instead of at the surface interface. This may result in detachment of fragments from one surface and attachment to the other surface. The surface often looks quite smooth when adhesive wear takes place. Abrasive wear occurs when a hard surface cuts material away from a

softer surface. This hard surface can also be wear debris. The surface generally looks quite rough when abrasive wear takes place.

Fatigue wear takes place due to repeated loading and unloading. Cracks occur after a while at the surface or underneath (subsurface). The cracks propagate and after a time particles from the surface may break out. A competition can exist between wear and fatigue: when the wear rate is high, fatigue cracks have no time to grow and simply wear away. This effect was also seen with head-hardened rails. Due to the increased hardness of the rails, the amount of adhesive and abrasive wear was reduced, resulting in more fatigue damage.

Plastic deformation is not a wear mechanism, but it is considered to be surface damage without loss of material [24]. The shape of a rail or wheel profile in this case is changed due to transfer of material to a different location.

Delamination wear can cause microscopic wear. If the plastic deformation surface layer is prevented, the wear rate is greatly reduced. In this type of wear, the surface of material is thought to be separated by the process of wear [47]. Delamination wear occurs in three steps by plastic deformation, germination of cracks and crack propagation. According to the delamination wear theory, the deformation of a plastic shape, crack formation and growth are created in a short depression of the surface that ultimately caused separation of sheets of wear particles.

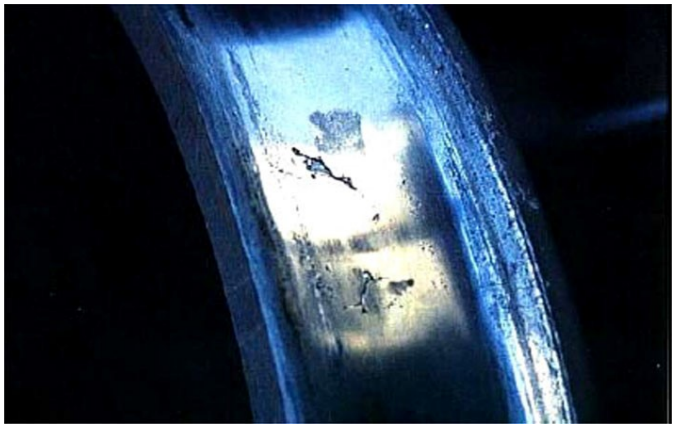

Fig. 2. 9. Delamination wear [33]

Fretting wear is caused when two surfaces would have tangential and oscillating movements under the applied loads with low relative amplitudes and the slip is caused by vibratory or cyclic stresses [48], [49] . This phenomenon is often associated with corrosion and oxidation [33]. As shown in

Fig. 2.10, observed by electron microscopy, fretting wear mechanisms are evident in four stages [46];

A. Adhesion and metal wear particles (Adhesive wear).

B. Creation of wear particles by mechanical–chemical effect. Mechanical action causes breaks off the oxide film and cleans the surface and strains of the metal, which is due to be active in the next half cycle, and the presence of this level in atmosphere causes oxidation (tribochemical wear).

C. Production of a uniform particle abrasion by fatigue (fatigue surface wear).

D. Wear oxide particles are created from the process as an abrasive powder and result in the ongoing destruction of the surface (abrasive wear). Among the factors affecting the deterioration due to fretting are the number of cycles, the range of motion, force, frequency, temperature.

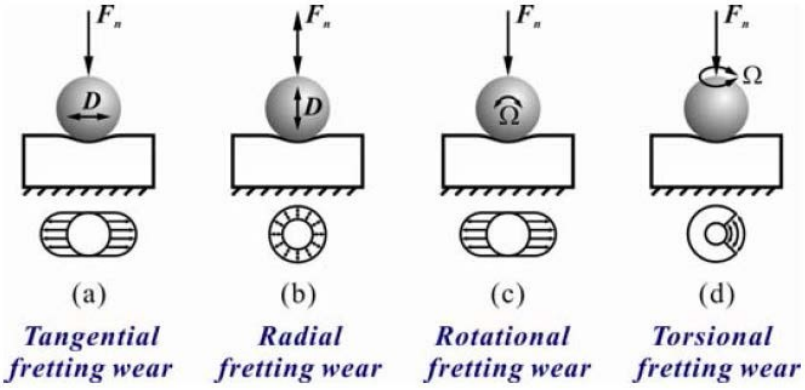

Fig. 2. 10. Mechanism of fretting wear [46]

Abrasive wear occurs when a hard surface is rubbed against a soft surface and by penetration, causing a track on the soft surface [33]. This type of wear is common in railway rails. The figure below depicts abrasive wear mechanism in railway rails. Abrasive wear mechanism as shown in figure below, follows different mechanisms.

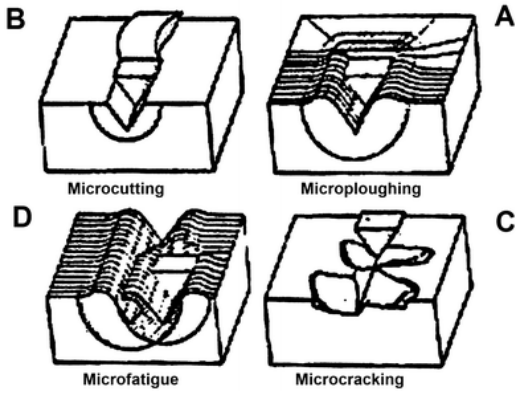

Fig. 2. 11. Abrasive wear mechanism [33]

The key indicator for this mechanism is a strain in a relatively large area around the surface tracks. In this case, scratches on the soft body would not scrape off the material, and the material only move on the surface and is regularly stored as a bulge on both sides of the created groove. Transfer of micro plowing mechanism to micro cutting takes place when the hardness of the material is increased. If the hardness of the sliding surface increases more and more, the abrasive wear can transform to micro cracking. In this mechanism, the particles are rubbed off due to the formation and growth phenomenon of a crack embedded in the grooves [33].

2.5. Contact Fatigue wear

Contact fatigue in wheel/rail tribology is as a result of the stress caused by the loading conditions in which the wheel and the rail are in sliding contact. This kind of wear is created with the formation of cracks and separation of material from the surface due to use of the repetitive alternating forces [48], [49] . The rotating contact or slipping can cause cycle stresses on the surface. Surface fatigue causes destruction of parts due to the alternative loading caused by the reaction of the components, and the destruction may begin with a defect or surface cracks [50] . The Fig. 2.12 shows the crack formation process for contact fatigue [33] .

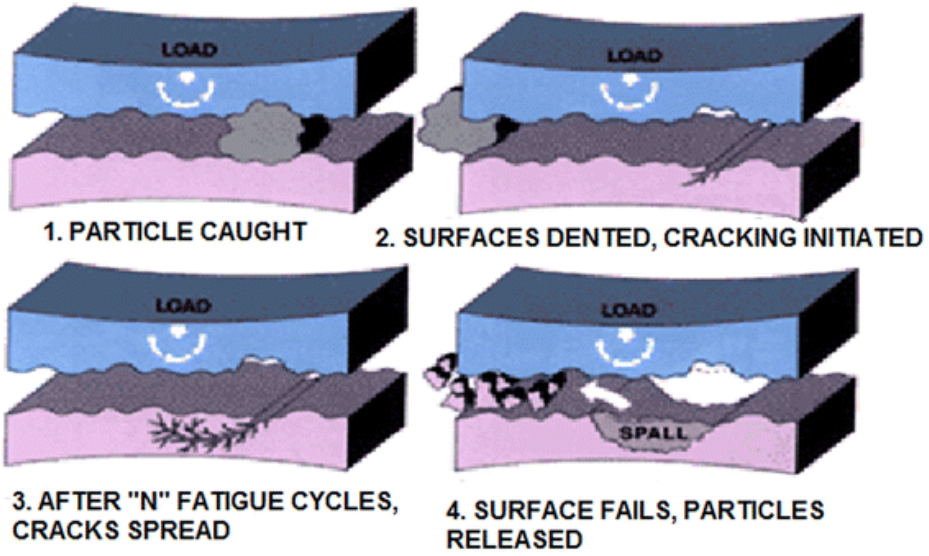

Fig. 2. 12. Surface contact fatigue mechanism [50]

2.6. Wear Tests

2.6.1. Rolling-lateral sliding wear test machine

Zakharov [51] conducted laboratory experiments on a rolling- lateral sliding wear testing machine in an unlubricated condition. Their laboratory experiment was carried out on wheel

flanges and on gauge lace of rail surfaces. They identified four wear modes (mild, severe, heavy and catastrophic) for the laboratory rolling- lateral sliding unlubricated wear tests. In their experiments, the wear rate was studied as a function of the TA/A parameter, where T is tangential force, A is the slide-to-roll ratio (creep), and A is the Hertzian contact area. They discovered that pA, where p is the contact pressure and A is the creep, is a more suitable parameter for the description of the wear modes and the wear mechanisms when the friction coefficient is stable.

2.6.2. JD-1 wheel/rail facility

The rolling wear tests of rail material was conducted by [21] using a JD-1 wheel/rail simulation facility under unlubricated condition. The JD-1 wheel/rail facility (as shown in fig. 22.) the experiment consists of host machine, hydraulic control system, electric control system, and data acquisition system. The tester is composed of a small wheel of diameter 62 mm that served as rail roller and a large wheel roller of diameter 1153 mm.

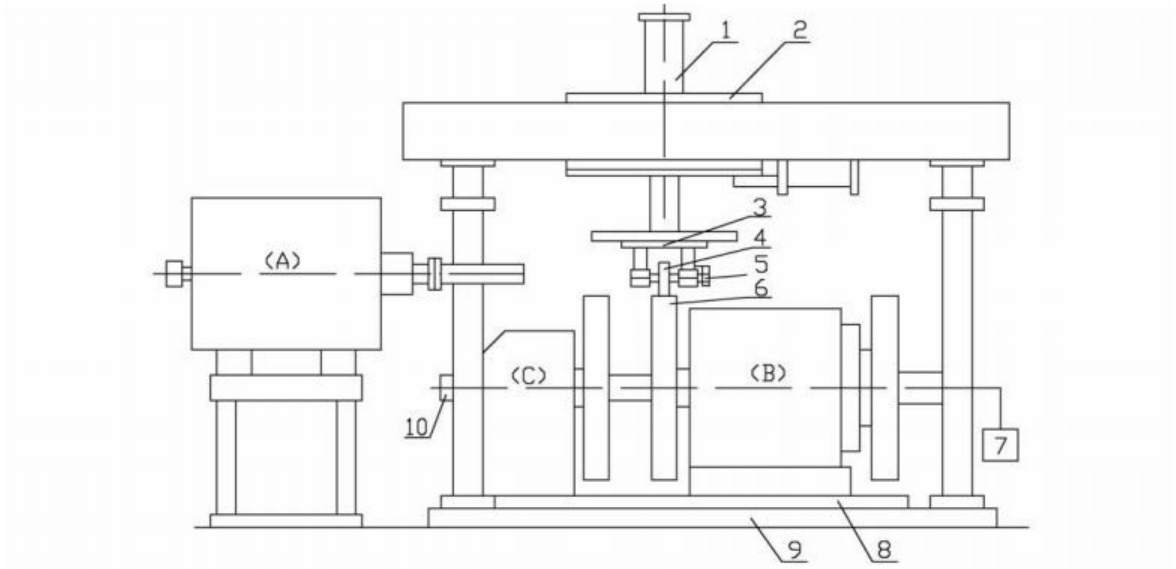

1 - Normal loading cylinder ;2 - Loading carriage ;3 - 3D load sensor ;4 - Rail roller ;5 - Brake system ; 6 - Large wheel roller ; 7 - Speed measuring motor ; 8 - Turning plate ; 9 - Base plate ; 10 - Optical shaft encoder

Fig. 2. 13. JD-1 wheel/rail facility [21]

They investigated the fatigue damage and wear behaviors of rail rollers by examining the micro-hardness, wear volume, and wear scars using optical microscopy and scanning electronic microscopy. His results indicated that wear volume of the rail roller increases rapidly with the increase of axle load and the decrease of curve radius of the rail. Also, he proved that when the rail wear is serious, the fatigue damage is relatively small and the relationship between fatigue crack damage and wear is a mutual competitive and restrictive coupling mechanism.

2.6.2. Nishihara type wear test machine

Honjo [29] conducted wear test on SP3 rail and conventional heat treated rail specimen using heat treatment method. They investigated the effect of wear resistance and RCF on the two rail specimen. Cylindrical wear test pieces with a diameter of 30 mm and thickness of 8 mm were taken from the rail head surface and a depth of 19.1 mm, and a wear test was performed. They used quenched and tempered steel with a Vickers hardness of HV370 as the simulated wheel material. The wear test was performed with a Nishihara type wear test machine under conditions of contact stress: 1.5 GPa, rotational speed : 800 rpm, slip ratio: –10%, and an non-lubricated environment. Their results showed that when the wear of the conventional heat-treated rail is assumed to be 100, the specific wear rate of the SP3 rail was reduced by 10% or more. This indicates that the SP3 rail has higher wear resistance and RCF resistance than the conventional heat treated rail and it can be used for heavy haul freight railways in North America and other countries.

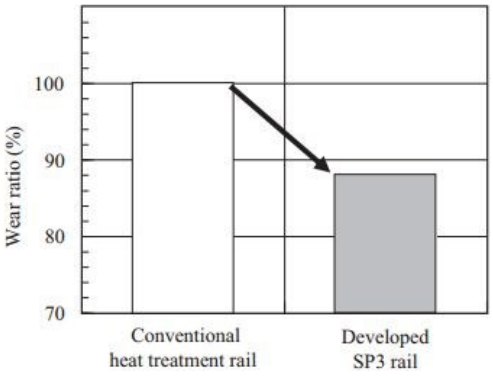

Fig. 2. 14. Comparison of wear resistance in actual track in service, between the conventional heat treatment rail and SP3 rail, taking 100 for wear loss in the conventional rail [29]

2.6.3. Pin on Disc Tribometer

Many researchers [52]–[55] has studied extensively on wear of rail materials using pin on disc Tribometer. [54] Studied on the wear of rails using a pin on disc Tribometers on normal loads in other to investigate the effect of applied load on wear mechanism and wear rate. He determined the wear rate using volumetric loss ($\pi \frac{D^2 H}{4}$) of the rail specimen. Rail steel used for the experiment are cut into pin and disc respectively. The disc samples are 42mm-1 in diameter and 5mm-1 in width and the pin samples are 6mm-1 diameter and 12mm-1 in length.

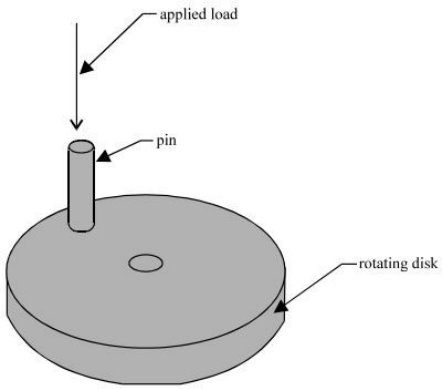

Fig. 2. 15. Pin on Disc setup [54]

The applied loads are 20N, 40N and 60N. The wear rate are calculated in unlubricated conditions for the samples and the wear test was performed with a speed of 100rpm. He used scanning electron microscope to determine the wear mechanism on the rail material From his experiment, it shows that wear rate increases linearly as the applied load increases and its proportionality coefficient is 0.1135. The coefficient of friction rail materials increases with the increasing of normal applied load (see fig. 2.15) and ploughing at higher load is responsible for higher values of coefficient of friction rail materials.

Viafara [52] studied the unlubricated sliding wear of pearlitic and bainitic steel rail materials. He noted that sliding wear has a great influence on the performance of wheel/rail materials, especially because the wheel flange slides over the rail in a curve track. He also noted that wheel/rail sliding introduces adhesive effects, high slip ratios strongly affect the rolling contact fatigue wear acting on the surfaces. He used AISI 15B30, 1070 and 1085 steels materials for his pin on disc wear test. After the steel specimen were heat treated, he then a sliding wear test were then conducted on the heat treated steel. The tribological pairs tested were AISI 15B30 bainitic and AISI 1070 pearlitic

pins sliding against pearlitic AISI 1085 disks. Loads of 10, 30 and 50N where applied at a maximum sliding distance of 3200m for pearlitic steel and 800m for bainitic steel pins and the sliding speed was 1m/s. Both disks and pins surfaces were polished with grade 600 silicon carbide emery paper before each test, in order to guarantee the same initial surface finishing conditions. Fig. 2.16 shows the variation of wear rates against normal load for pearlitic AISI 1070 and bainitic AISI 15B30 pins. He concluded that the wear rate of bainitic pins increased continuously with normal load and the measured values were at least two orders of magnitude greater than those found for pearlitic pins. The wear rate of bainitic pins increased continuously with normal load and the measured values were at least two orders of magnitude greater than those found for pearlitic pins.

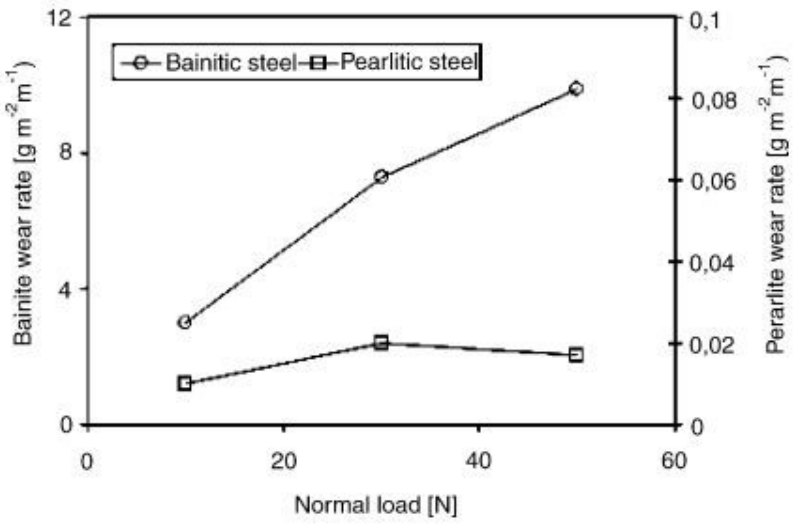

Fig. 2. 16. Wear rate as a function of the normal load for pearlitic and bainitic pins [52]

2.7 Wheel/rail materials

This section will give an overview of steel materials used for railway rails and their chemical compositions. Rails are grouped according to their standards, strength, grade, quality and length. The rail steel qualities can be distinguished in to two categories [7]; Normal steel quality with an ultimate tensile strength of 700-900 MPa and hard steel quality used mainly on curves, and crossings etc. with an ultimate tensile strength of 900-1200 MPa.

Rails differ greatly in their chemical compositions such as carbon, manganese, chromium and silicon which varies depending on their requirements. Since the rails have to withstand the impact

load, friction and stress of freights, they should have sufficient strength, hardness, toughness and good welding performance [7]. However a large increase in rail mechanical strength may result brittle failure and as a result a further increase is not desirable.

There are different types of wheel/rail materials used around the world of railways for different applications. Wheel/rail materials are quite similar in composition, differing slightly in the amounts of carbon, silica, and manganese in the steels used.

Table 2.1 reports different chemical composition of rail materials that has been used for carrying out wear test.

Table 2. 1. Different wheel/rail material used in Railways

Researchers	Chemical composition of studied rail materials (%wt) except boron								
[21]	**Rail**	**C**	**Si**	**Mn**	**S**	**P**	**V**	**Cr**	**Fe**
	PD3 U71 Mn	0.793	0.712	0.771	0.793	0.014	0.022		
		0.736	0.282	1.4	0.736	0.033	0.02		
[29]	SP3 Rail	0.81	0.55	0.55	0.005	0.014	others		
[54]			0.02	0.01	0.05	0.45			Balance
[55]		0.778	0.229	1.018	0.023	0.022			

2.8. Wear Models

Several authors [15], [20], [63]–[68], [22], [56]–[62] has researched on the wear models of different materials. Wear has been known to many researchers to be due to loss of oxide [69], no models covering this mechanism, other than that of [67]have appeared of late.

Bahadur [66] summarized a workshop in the 1977 Wear of Materials (WOM) conference while Barber [70] stated that the general philosophy of modeling. He opined that "Engineering modeling rests on the premise that even the most complex engineering system can be conceived as consisting of an assembly of relatively simple components whose instantaneous state is describable in terms of a finite number of parameters and whose subsequent behavior

depends upon interaction with its neighbors through mathematically quantifiable physical laws“ . Barber’ s description of modeling is clearly based on systems that can be modeled as a set of discrete mechanical units. [69] in his paper focuses on the need for new methods and offers recommendations on how to model the wearing process.

Archard in his 1953 study used a simple model to compare the deduced theory (the deduced dependence of the experimental observables on the load) with the experimental evidence. From his study, he suggested that the most realistic model is one in which increasing the load increases both the number and size of the contact areas and the mechanical wear should also depend on the model. However, in wear his experiments, he showed that the wear rate is proportional to the load, and the results can be explained by assuming removal of lumps at contact areas formed by plastic deformation which suggests that a basic assumption of previous theories, that increasing the load increases the number of contacts without affecting their average size, is redundant

2.8.1. Wear Equations

Many equations has been derived using the method of solid mechanics to investigate the wear rate. Most include material properties, thermodynamic quantities or other engineering variables [69]. Rhee [71] studied the wear of polymer materials sliding against metal surfaces. He discovered that the total wear of the polymer depends on speed V, time t, and applied load F according to the equation;

$$\Delta W = KF^a V^b t^c \qquad \text{Eq. 1}$$

Where ΔW is the weight loss of the polymer material and K, a, b and c are empirical constants.

In his wear experiment, the wear volume variation is measured when either V, F or t is varied in turn and two of the variables are fixed.

Barwel [72] in his paper suggested that wear rates may be typified by one of three curves of the type;

$$V = \frac{\beta}{\alpha}[1 - \exp(-\alpha t)] \qquad \text{Eq. 2}$$

$$V = \alpha t \qquad \text{Eq. 3}$$

$$V = \beta \exp(\alpha t) \qquad \text{Eq. 4}$$

where V is the volume loss, α is constant and t is time.

The parameter β is some characteristics of the initial surfaces.

Archard [73] in his experiment discovered that the worn volume V depends on the sliding distance S, the applied load P and flow pressure P_m (approximately equal to the hardness) of the softer material.

$$V = KS\,\frac{P}{P_m} \qquad \text{Eq. 5}$$

Where $\frac{P}{P_m}$ is known as the real contact area and K is a constant related to the probability that an encounter of two asperities will produce a wear particle. However the value for K is obtained from experiments and is also known as wear coefficient.

Few researches have been done on the area of rail wear in AALRT, especially when we come to wear caused as a result of wheel/rail interaction, hence, there is a huge gap of research that needs to be filled. Therefore this study is expected to give a start to filling this gap in this research area. Finally, in this paper, wear analysis will be conducted using SIMPACK to investigate the wear behavior of rails of AALRT. The main issues here are safety, comfort and minimizing cost of maintenance and operation.

Chapter three

3. Materials and Method

3.1 Operational parameters of Addis Ababa Light rail transit and train

Addis Ababa light rail transit consist of East-west and South-north lines in Addis Ababa (Phase I) with total length of main lines around 31.025km, where the East-west main line is around 16.998km long; the South-north main line is around 16.689km long. Both lines share the same section of around 2.662km in the urban areas. Vehicles are 70% low floor modern trams with maximum operating speed of 70km/h and average travelling speed of 20km/h (average dwelling time of 30 seconds at each station). The line uses a track gauge of 1435mm and a standard rail type of 50kg/m with axle load of ≤11（1+3%）t. The table 3.1 shows the technical specifications of the vehicle used in AALRT and fig. 3.1 shows a vehicle on AALRT on a rail.

Table 3. 1. Main dimensions of vehicle for AALRT

	Technical parameters	Value
1	Vehicle length	30000 mm
2	Maximum width of car body:	2650mm
3	Wheel diameter (new wheel)	660 mm
4	Wheel diameter (Max. wear)	600 mm
5	Seating capacity (AW_2) (standing: 6 persons/m^2)	254
6	Overload capacity (AW_3)(standing: 8 persons/m^2)	317
7	Empty vehicle (t)	44
8	Seating capacity (t)	59.24
9	Overload capacity (t)	63.07
10	Minimum radius of vertical curve (m)	1000
11	Maximum speed(Km/h)	70

12	Maximum gradient	55%
13	axle load (t)	≤11 （1+3%）
14	Wheelset mass	880 Kg
15	Wheel set moment of inertia	Ix = 176 kg m^2 Iy = 76 kg m^2 Iz = 176 kg m^2

Note: Taking 60kg as average weight of each passenger.

Source: Ethiopian Railway Corporation technical vehicle specifications

Table 3. 2. Environmental Condition in Addis Ababa Region

Altitude	2500m
Ambient temperature	0℃ +29.7℃
Average daily highest temperature in years:	25.5℃
Average daily lowest temperature in years	6.1℃
Average relative humidity in year	95%
Average annual rain fall	1000-1600mm
Maximum daily rain fall	47mm

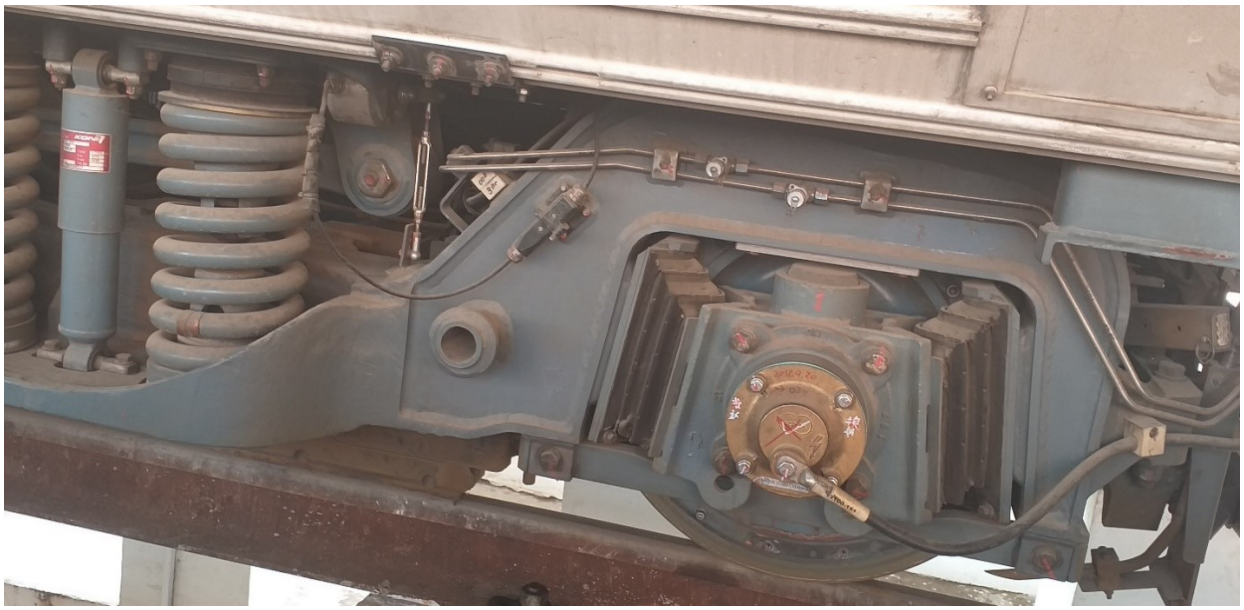

Fig. 3. 1. AALRT vehicle wheel on rail

3.1.2. Materials used for the study

The materials used in this study are railway steels. The chemical composition of the railway steel is shown in the table 3.3 while the mechanical properties is shown in table 3.4. The rail type used is UIC 50 rail. Table 3.5 shows the wheel/rail parameters for AALRT. The rail is designed as a beam with the cross section of a UIC 60kg/m standard rail.

Table 3. 3. Chemical compositions of the rail material

Rail material (%)	**C**	**Si**	**Mn**	**P**	**S**	**Ni**	**Cr**
	0.8	0.28	1.00	0.04	0.05	0	0

Source: Ethiopian Railway Corporation technical vehicle specifications

Table 3. 4. Mechanical properties of the rail material

	Mechanical property	**Value**
1	Young's modulus	207GPa
2	Density	7800kg/m^3
3	Ultimate tensile strength	880 MPa
4	Yield strength	640MPa
5	Poisson's ratio	0.3
6	Elongation	>10%

Source: Ethiopian Railway Corporation technical vehicle specifications

Table 3. 5. Wheel/Rail parameters for AALRT

Parameters	**Dimension(mm)**
Height of rail	152
Width	125
Height of rail head	49.4
Width of rail head	72.2
principal rolling radii of the wheel	R_{1y}= 330 mm
principal transverse radii of the wheel	R_{2y}= ∞
principal rolling radii of the rail	R_{1x}= ∞

principal transverse radii of the rail	R_{2x} = 300 mm

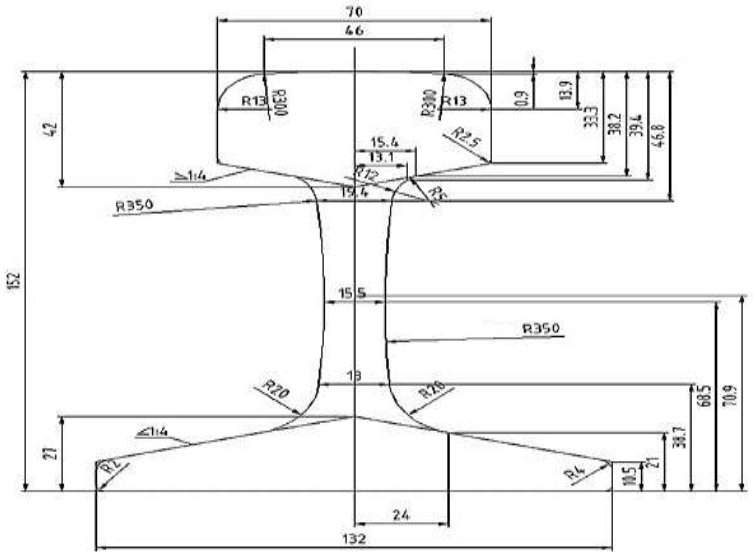

Fig. 3. 2. Cross section of Addis Ababa light rail

Source: Ethiopian Railway Corporation technical vehicle specifications

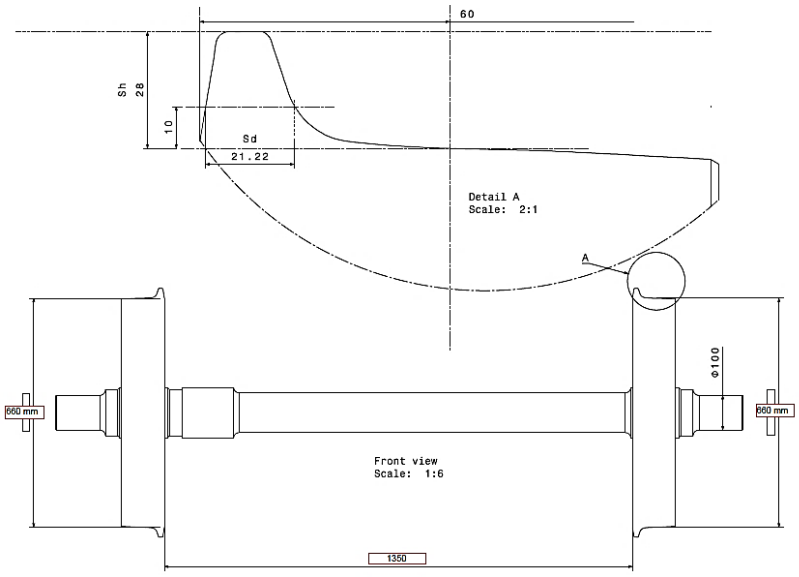

Fig. 3. 3. Wheel Dimension for AALRT Vehicles

Source: Ethiopian Railway Corporation technical vehicle specifications

The table 3.6 shows the angular velocity for AALRT vehicle.

Table 3. 6. Angular velocity for AALRT vehicles

	Linear velocity (Km/hr.)	**Angular velocity (rad/s)**	**RPM**
Maximum operating speed	70	58.92	562.65
Average travelling speed	20	16.84	160.81

3.2. Numerical Analysis

In this section, a numerical investigation will be carried out using SIMPACK software. SIMPACK is a multi-body simulation package that can used to investigate, simulate and model complex railway vehicle components, such as railway wheels, bogie, etc. It can be used to predict and optimize the behavior of the railway vehicle components using different integration techniques. With SIMPACK both online and offline time integration can be done on the rail vehicle component to generate different results such as, creepages, creep forces, wear number etc. finally, wear rate, wear volume and were derived and determined.

3.2.1 Modelling of the rail vehicle on rail

The input parameters for modelling is given in table 3.1 to 3.6. The model of the wheel on rail is illustrated in fig. 3.4. In other to solve the model, the simulation is done for about 20 seconds (since the results does not change significantly with time). The output steps is taken as sampling rate and the integration method is the Jacobian evaluation.

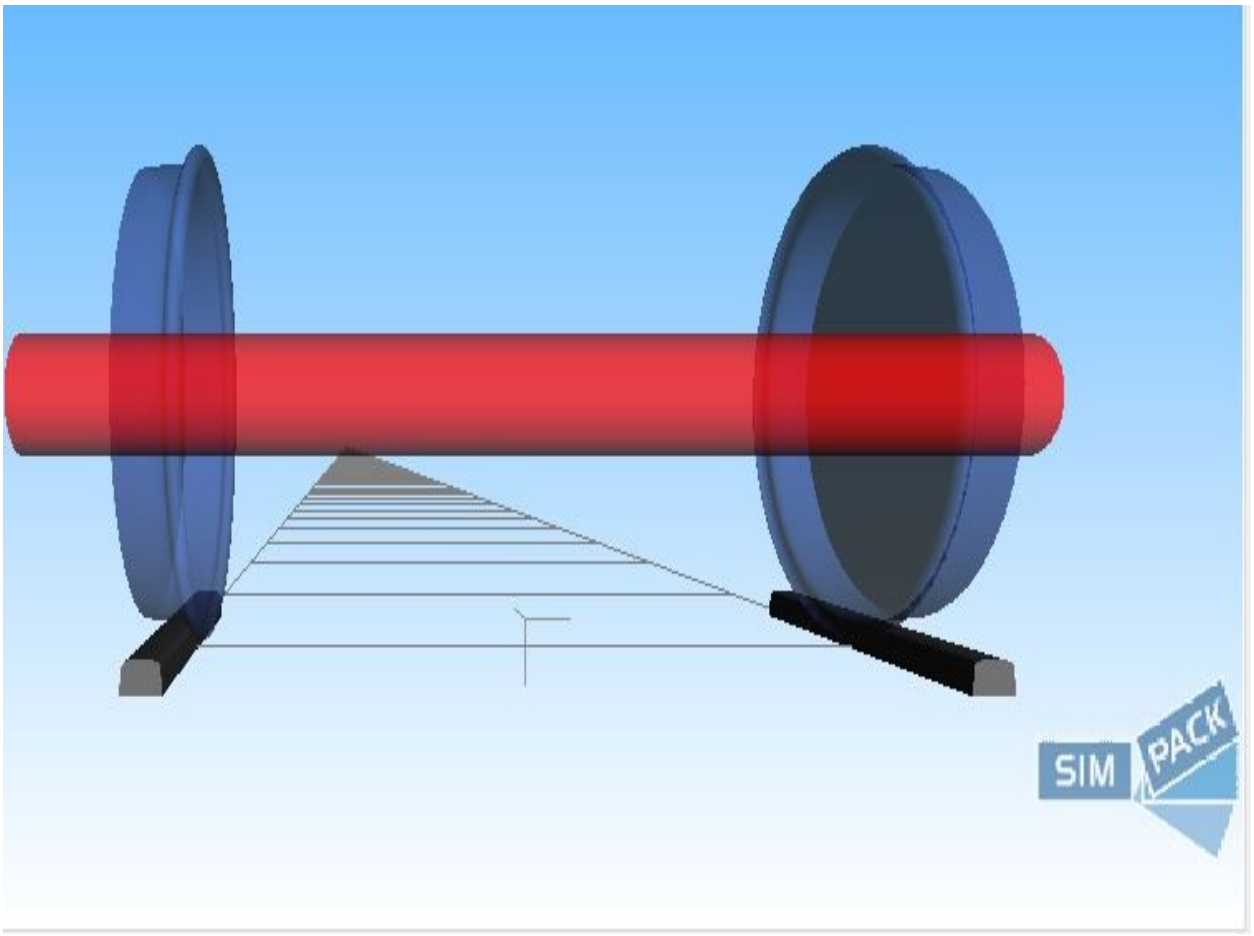

Fig. 3. 4. Model of wheel on Rail

3.2.2 Assumptions during simulation

- Track irregularity is not included so regular standard track is considered
- Wheel profile of the wheels are considered identical
- Simulation is done for different values of coefficient of friction (0.1, 0.2, 0.3, 0.4, 0.5)
- Simulations is done for three different capacity of the train capacity (empty, seating and overload capacity of the train).
- Simulation is done for different range of speed of the train (20 Km/h to 70 Km/h)
- Simulation is done only for the straight track section of AALRT, the curve portion is not considered.

3.3. Hertzian theory for 3D wheel/rail contact

In order to Study the contact between bodies the first thing to do is to determine some contact parameters: the contact surface, the pressure and the tangential forces.

Two contacting surfaces under load will deform (plastic or elastic) In many engineering applications: rolling contact bearings, gears, cams, wheel/rail contact etc. , the contact surfaces are non-conformal (very small contact area and high pressure). It is essential to know the values of stresses acting in such contacts based on the theory of elasticity (analytical formulae) called Hertzian equation which was developed by Hertz in 1880 during his Christmas vacation.

Hertz's model of contact stress is developed based on the following assumptions:

- The materials in contact are homogeneous and the deformation is elastic
- The effect of surface roughness is negligible and smooth
- Contact stress is caused by the load which is normal to the contact tangent plane which effectively means that there are no tangential forces acting between the solids
- The contact area is very small compared with the dimensions of the contacting solids
- The contacting solids are at rest and in equilibrium.
- The surfaces of the bodies are represented by quadratic functions in the vicinity of contact. In other words, the curvatures of the surfaces in contact are constant [74]

Hertz made the hypothesis that the contact area is, in general, elliptical, by his observations of interference fringes.

If two elastic nonconforming bodies contact together then according to the Hertz contact theory, the contact area is elliptical in shape with a major semi-axis a and a minor semi-axis b [75]. If we consider the wheel and rail to be an elastic material in contact, they will meet at a single point O, where the normal distance between them is zero. Near this contact point, without load, the body surface shapes may be represented by two second-order polynomials

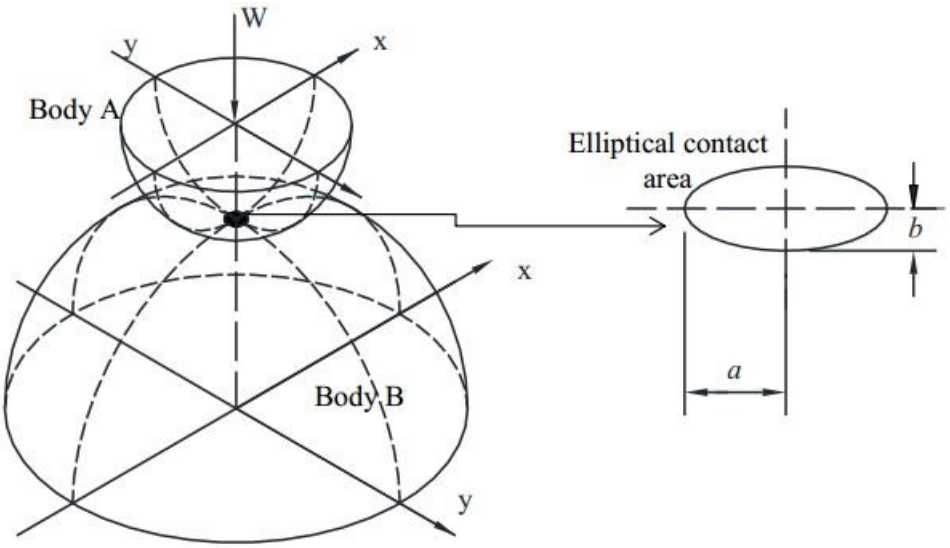

Fig. 3. 5. Two elastic bodies with convex surface in contact [75]

Hertz proposed the solution for the determination of contact area and pressure distribution between two bodies in contact. The body surface shapes near the contact point without load may be represented by the Eq.6 and Eq.7 below.

$$Q_1(x,y) = A_1X^2 + B_1Y^2 \quad \text{Eq. 6}$$

$$Q_2(x,y) = A_2X^2 + B_2Y^2 \quad \text{Eq. 7}$$

The coefficients A_1, A_2, B_1 and B_2 are constants, with A_2 equals to zero since the railway track is practically straight. So therefore,

$$A = \frac{1}{2}\left(\frac{1}{R_{1y}} + \frac{1}{R_{2y}}\right) \quad \text{Eq. 8}$$

$$B = \frac{1}{2}\left(\frac{1}{R_{1x}} + \frac{1}{R_{2x}}\right) \quad \text{Eq. 9}$$

Where, $R_{1x}\ and\ R_{1y}$ are principal rolling radii of the rail and wheel respectively and $R_{2x}\ and\ R_{2y}$ are principal transverse radii of curvature of the rail and wheel respectively. The pressure over the contact patch is given as,

$$P(x,y) = P_o\sqrt{\left(1 - \left(\frac{x}{a}\right)^2 + \left(\frac{y}{b}\right)^2\right)} \quad \text{Eq. 10}$$

where a is the longitudinal semi axes of the contact ellipse and b is the lateral semi axes of the contact ellipse, F is the vertical load applied normal to the contact patch, and $P_{max} = \frac{3F}{2\pi ab}$ is the maximum contact pressure (Hertz contact pressure) which occurs at x=0 and y=0. To find the value of a and b we used Eq. 11

$$\cos\theta = \frac{|A-B|}{A+B} \quad \text{Eq. 11}$$

$$a = m\left[\frac{3}{2}\frac{F(1-v^2)}{E(A+B)}\right]^{\frac{1}{3}}, \text{ and } b = n\left[\frac{3}{2}\frac{F(1-v^2)}{E(A+B)}\right]^{\frac{1}{3}} \quad \text{Eq. 12}$$

Where, E is the modulus of elasticity and Poisson's ratio, assuming the same material for the rail and wheel and m, n, are non-dimensional coefficients as shown in Appendix B

Calculating for the value of angle (θ), we first find A+ B and $|A-B|$ below,

$$A+B = \frac{1}{2}\left(\frac{1}{R_{1y}}+\frac{1}{R_{2y}}\right) + \frac{1}{2}\left(\frac{1}{R_{1x}}+\frac{1}{R_{2x}}\right) = 0.003165\ mm^{-1}$$

$$|A-B| = \frac{1}{2}\sqrt{\left(\frac{1}{R_{1y}}-\frac{1}{R_{2y}}\right)^2+\left(\frac{1}{R_{1x}}-\frac{1}{R_{2x}}\right)^2+2\left(\frac{1}{R_{1y}}-\frac{1}{R_{2y}}\right)\left(\frac{1}{R_{1x}}-\frac{1}{R_{2x}}\right)\cos(2\gamma)} \quad \text{Eq. 13}$$

Where, γ is the straight segment curvature of the rail, which is usually equals to the value of45^o.

$$|A-B| = 0.0022524\ mm^{-1}$$

$\cos\theta = 0.7117$, and $\theta = 44.63^o$

By interpolating values of m and n from appendix B. Above, we have,

$m = 2.156\ and\ n = 0.564$

The values for a and b can then be gotten from Eq. 12.

To find the contact pressure, we need to find the vertical wheel load applied to the contact patch at different carrying capacity.

Empty weight of the vehicle = 44 t = 431640 N

Seating capacity of the vehicle = 59.24 t = 581144.4 N

Overload capacity of the vehicle = 63.07 t = 616716.7 N

Each vehicle in AALRT has 3 cars and each car has one bogie and each bogie has 4 wheels, so each vehicle has 12 wheels. The normal load applied by the vehicle on each wheel is given below;

For empty vehicle = 35970 N

For seating capacity of the vehicle = 48428.7 N

Overload capacity of the vehicle = 51392.23 N

Chapter 4

4.0. Result and Discussion

4.1. Analytical Results

Wear is the gradual damage between materials involved in relative motion. For an unlubricated sliding condition such as the wheel or rail, the wear rate depends on the normal load, relative sliding speed, initial temperature and the thermal, mechanical and chemical properties of the material in contact [45]. Some of the factors that affect wear of rails are wheel load, speed, adhesion, material type etc. but for the purpose of this analysis, we shall be considering the effects of speed and wheel load on the wear of the rail material.

The normal load applied by the vehicle on each wheel and the values of *a, b*, P_{max} and *Po* (mean contact pressure, 0.78 P_{max}) is tabulated below;

Table 4. 1. Values of contact patch parameter (a, b, P_{max}, Po)

Lording condition	Cases	Load (N)	a (mm)	b (mm)	P_{max} (MPa)	Po (MPa)
Empty vehicle	1	35970 N	9.09	2.38	793.85	619.203
Full capacity	2	48428.7 N	10.04	2.63	875.69	683.04
Overload capacity	3	51392.23 N	10.24	2.68	894.14	697.43

It can be seen from table 4.1 that as the loading capacity of the train increase, the mean contact pressure also increases. This increment has an adverse effect on the rail, as it increases the wear rate of the rail. So in order to to reduce the wear on the rail, the train must be loaded to a reasonably capacity.

4.2. Numerical analysis result and discussion

In this research work the effect of loading conditions, running speed and coefficient of friction on the wear parameters of rails of Addis Ababa light railway were investigated. The results of the simulation will be given in specific wear rate (mm^3/N m) instead of wear rate (volume loss per unit sliding distance, mm^3/m) since wear rate is load independent and also Specific wear rate is more accurate description of the wear characteristics of any materials, particularly for steel

materials[76]. It is used as a precise indication of the wear properties of the sliding bodies under Loads, speeds, and sliding distance or time. Simulation of vehicle model is conducted using SIMPACK. The model was simulated for about 20 seconds with different maximum mean Hertzian pressure of: 619.203 MPa, 683.04 MPa and 697.43 MPa and sliding distance of 111.2 m, 194.4m and 388. 9 m. All The results of the numerical solution can be found in appendix A. here the effect of friction, loading conditions and speed on wear rate are summarized.

4.2.1. Effects of vehicle load on wear rate of rails

Fig. 4.1 represents the specific wear rate versus coefficient of friction at different capacity of the train.

Where,

Case 1 = empty train capacity

Case 2 = seating capacity of the train

Case 3 = overload capacity of the train

a)

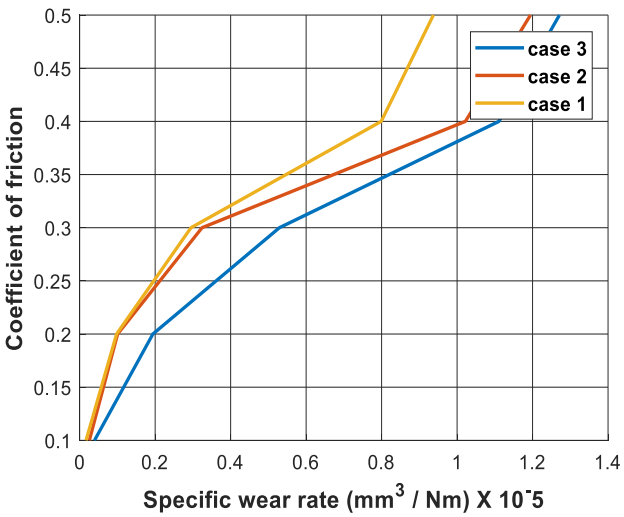

b)

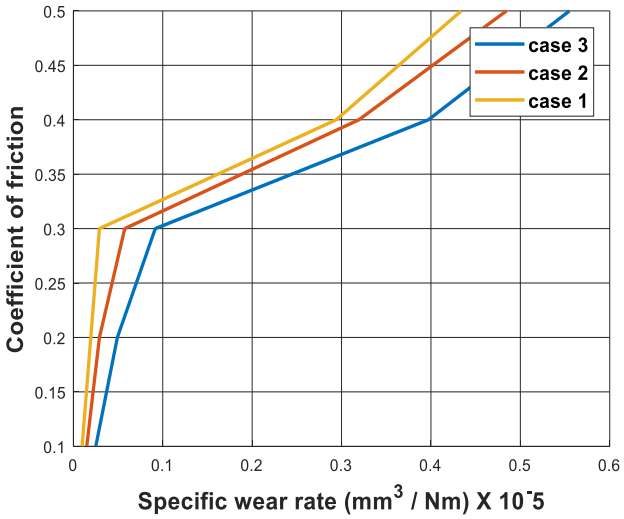

c)

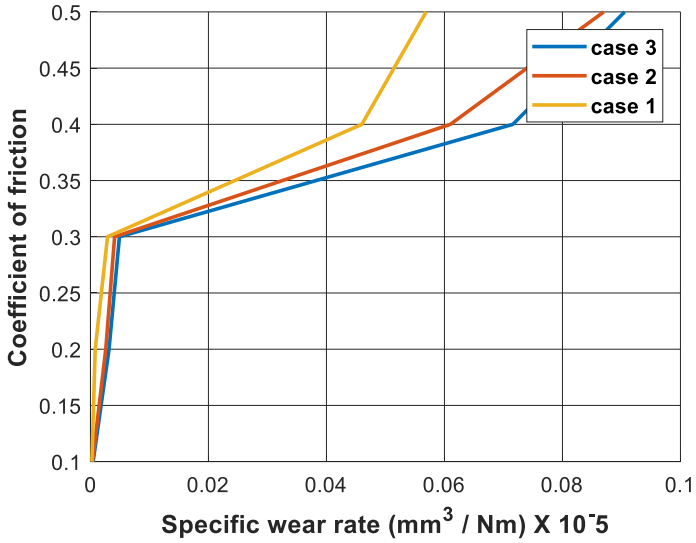

Fig. 4. 1. a) Specific wear rate against coefficient of friction at 70 Km/hr running speed of the train
b. Specific wear rate against coefficient of friction at 35 Km/hr running speed of the train
c. Specific wear rate against Coefficient of friction at 20 Km/hr

The wear rate significantly increases as the coefficient of friction between the train wheels and rails increases. In addition to the small coefficient of friction variation, loading conditions variation affects the specific wear rate. As the load increases from empty to overloading cases, the wear rate increases. From the fig. 4.1a to c, it can be seen that the trends are similar for the rest of selected vehicle speed cases. For the 20Km/hr vehicle speed, the specific wear rate increase slightly until the COF is 0.3 afterwards, it increases significantly until the COF is 0.4, and then the increment is at the continuous. For the 35 Km/hr vehicle speed, the trend is almost similar with the 20 Km/hr case. For the 70 Km/hr case, the specific wear rate increases almost linearly till it reaches a COF value of 0.4, after which, there is a sharp increment upwards. This results tends to agree with the work done by [77] on the effects of vehicle load on wear rate. From his work, as the applied load increases, the wear rate increases and vice versa.

4.2.2. Effects of Vehicle speed on wear rate of rails

The wear rate due to time increases slightly as vehicle speed increases. This is due to the changes coming from friction heating between the wheels and the train.

a)

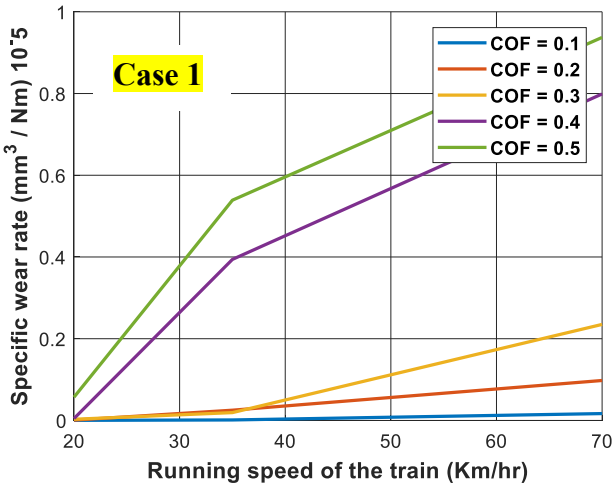

b)

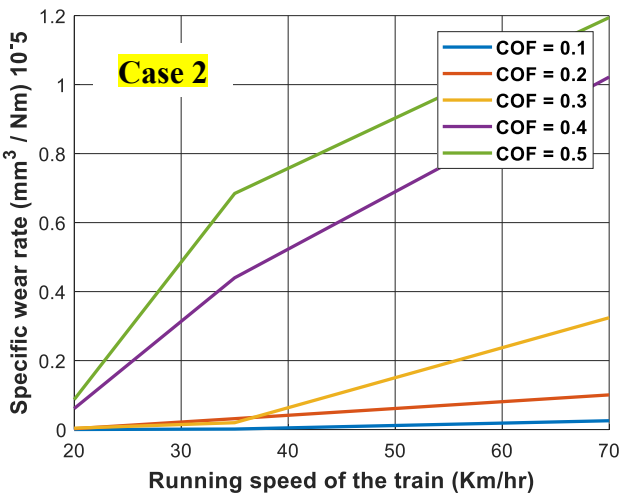

c)

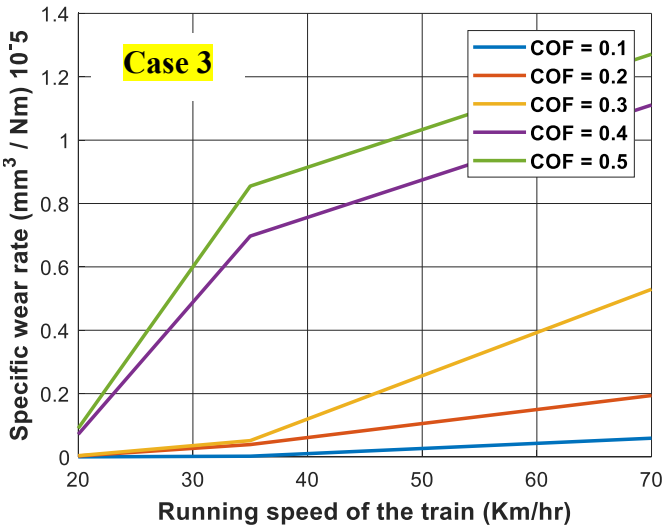

Fig. 4. 2. Specific wear rate against Vehicle speed

From fig. 4.2a to c, the variation of specific wear rate against running speed of the train follows similar trends. It can be seen that there is a slight increment in the specific wear rate for coefficient of friction values of 0.1, 0.2 and 0.3 but as the COF exceeds 0.3, the specific wear rate becomes very high, this is due to the fact that there is an increment in vehicle speed. When the coefficient of friction is constant, as the speed increases, the specific wear also increases and vice versa. It is worthy to note that as the vehicle speed and COF increases, the Specific wear rate increases, thus maintaining appropriate vehicle speed and normal wheel load levels can reduce coefficient of

friction and in turn reduce wear and improve the railway rails. According to [78], in his experiment of unlubricated sliding for AISI 1045 carbon steel pins, he opined that the specific wear rate are categorized into two groups namely; mild and severe wear type. For the mild wear type, the specific wear rate is in the range of (10^{-7} to 10^{-4} while the severe wear type is in the range of 10^{-3} mm^3/Nm). He agreed that the specific wear rate decreases with a decrease in speed. This result tends to agree with his in the sense that the specific wear rate of the AALRT rails is in the range of 10^{-5} mm^3/Nm.

4.2.3. Effects of Vehicle wheel load on wear rate of rails

From fig. 4.1a to c, it can be seen that, the wear rate reduces as the applied wheel load reduces. It reduces by a magnitude of 10^{-1}, the highest specific wear rate is recorded at a COF of 0.5 for the overload capacity when the vehicle is running at its maximum operating speed while the lowest specific wear rate is recorded at a COF of 0.1 when the vehicle is running at 20 Km/h.

4.2.4. Effect of sliding distance on volumetric loss of rails

The volumetric loss of the rail material reduces as the sliding distance reduces and increase as the sliding distance increase. From fig. 4.3a and fig. 4.3b, it can be seen that as the coefficient of friction increases, the curve becomes more linear, this is due to the high velocity values. The values for the volumetric loss can be found in appendix C. This results tends to agree with that of [21] in his experiment involving the investigation of wear properties of rails. He agree that the wear volume of the rail roller increases rapidly with the increase of axle load.

a)

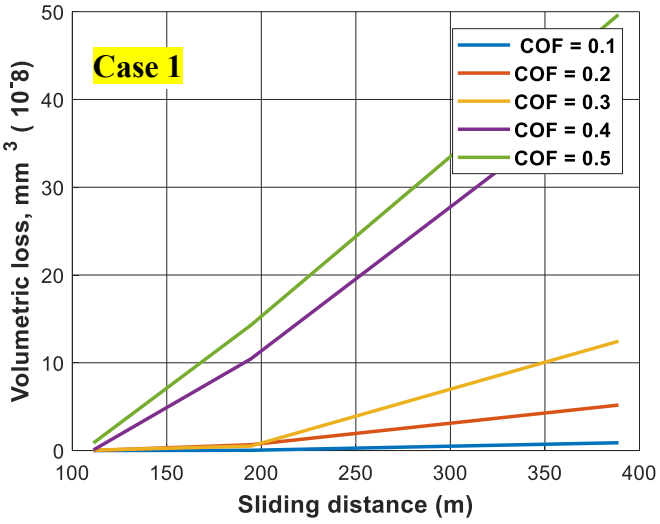

b)

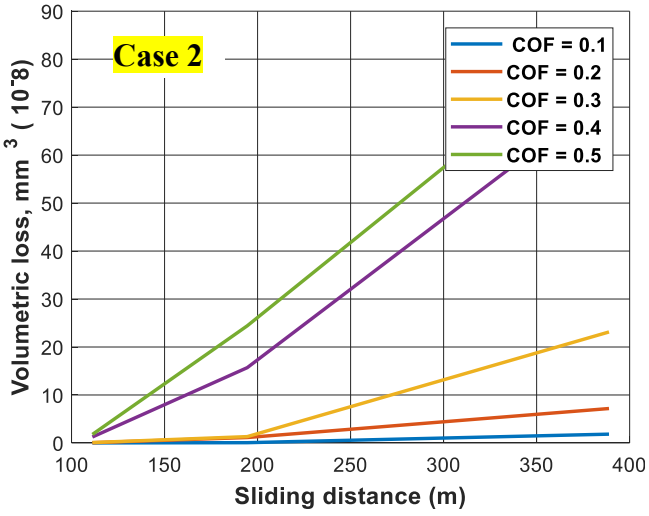

c)

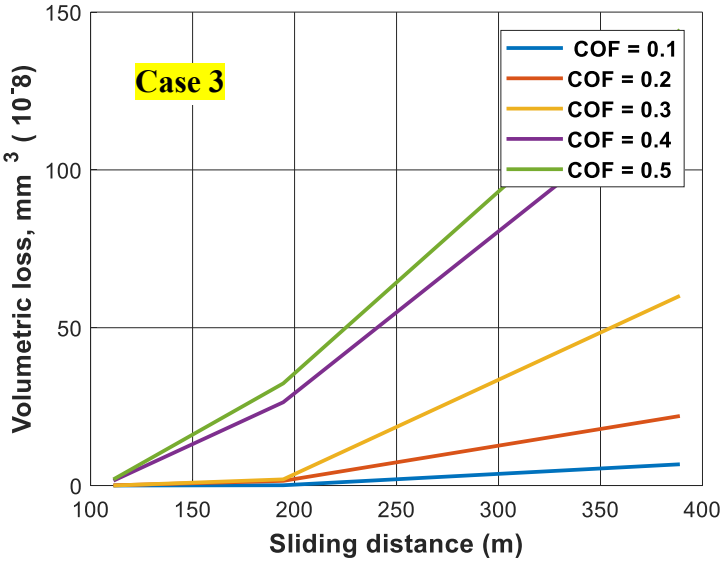

Fig. 4. 3.Volumetric loss at different loading conditions of the train

4.2.5. Effect of sliding distance on Wear rate of rails

a)

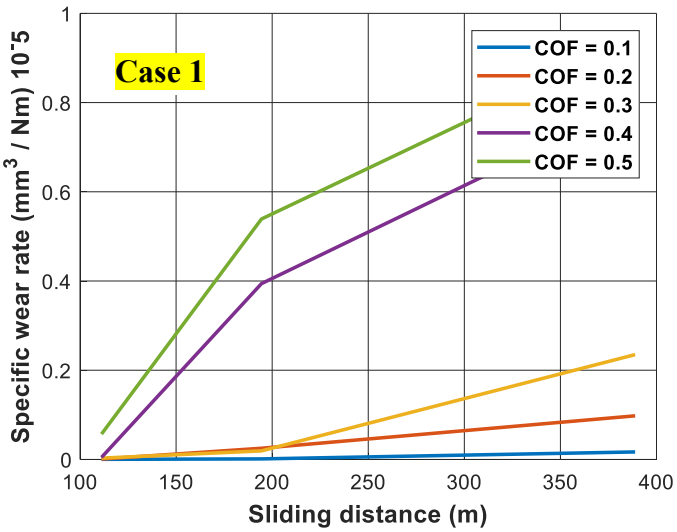

b)

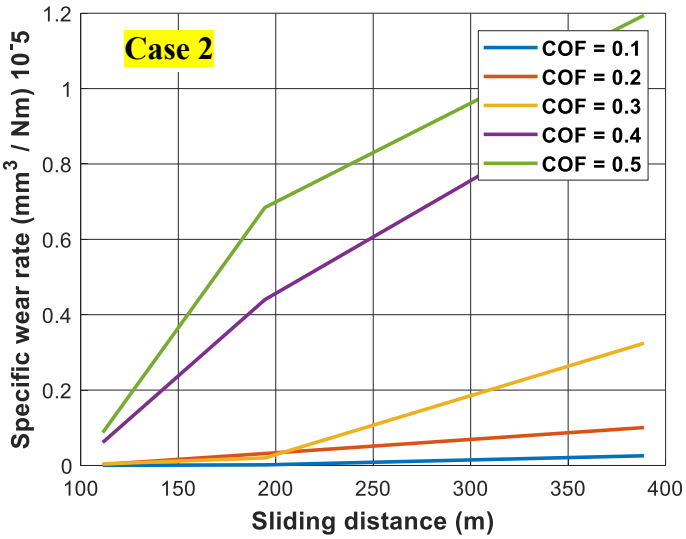

c)

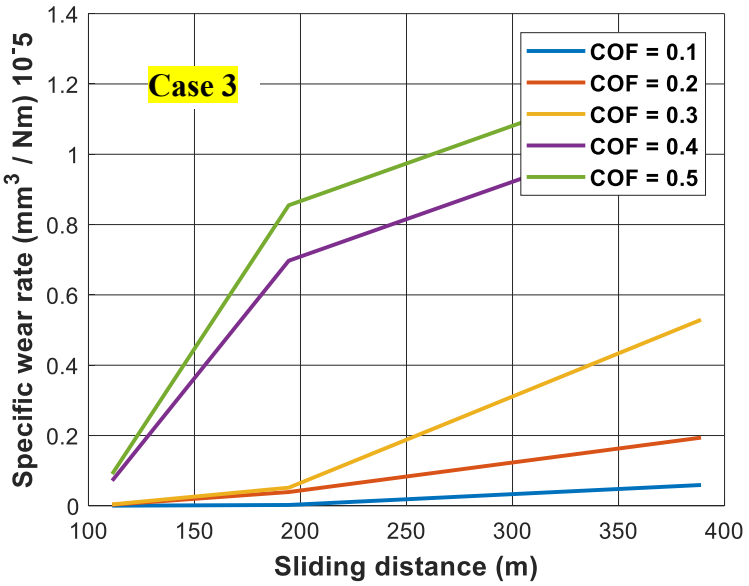

Fig. 4. 4. Effect of different loading conditions and sliding distance on wear rate

Fig. 4.4a to c shows the effect of sliding distance on the specific wear rate of the rail. In Fig. 4.4a, the sliding distance at which the specific wear rate was maximum was at 388.9 m and the sliding distance at which the specific wear rate was minimum was at 111.2 m. This shows that as the sliding distance increases, the specific wear rate increases and vice versa. As the loading capacity of the train increases, the curves dips outwards as shown in Fig. 4.4c. The coefficient of friction has an effect on the sliding distance as it affects the specific wear rate of rails. At higher sliding distance, the specific wear rates increase and at lower sliding distance, the specific wear rate reduces. According to the wear studies by [46], [78]–[80], they all agreed that the wear performance of steel materials deteriorates with increase in the sliding distance which validates the results in this study.

4.3. Result comparison

The result in this study is in agreement with work the done by Windarta, 2011 [81] and also with the study done by Kato, 2011 [78] on the friction and wear of passive metals and coatings. The contact pressure result is also in line with the work of Pau, et al., 2002 [63].

Chapter 5

5.0. Conclusion and Recommendation for future work

5.1. Conclusion

The wear behavior of Addis Ababa light rail transit rails was studied. The effects of coefficient of friction, wheel load and vehicle speed was investigated. The following conclusions was drawn on completion of the research;

- ✓ The highest specific wear rate occurred at the maximum operating speed of the train (70 Km/hr.) while the lowest specific wear rate occurred at a speed of 20 Km/h. this shows that as the running speed of the train increases, the specific wear rate increases.
- ✓ The highest wear rate of the rail occurred at the overload capacity of the train.
- ✓ The specific wear rate of rails slightly increases as the coefficient of friction increases.
- ✓ The coefficient of friction has an effect on the sliding distance as it affects the specific wear rate of rails. At higher sliding distance, the specific wear rates increase and vice versa.
- ✓ The lower the running time of the train, the lower the specific wear rate of the rail.
- ✓ At constant coefficient of friction. As the wear rate is reducing, the volumetric loss is increasing.
- ✓ The wear rate of rails reduces as the applied wheel load reduces. So in other to increase the wear life of the rails, it is imperative to use medium friction coefficient values and operate the train between the speed ranges of 20 to 40 Km/hr.

5.2 Recommendation

The specific wear rate significantly increases as the wheel load increases. Also, small coefficient of friction values, together with increase in vehicle speed, wheel load and sliding over long distances, reduces wear rate. So by maintaining appropriate train speed within the range of 20 to 40 Km/hr and by using small coefficient of friction values we can reduce frictional force and wear and also improve railway infrastructure, thereby making last for the required duration.

5.3. Future work

Railway tribology is an interesting field to be studied. I encourage future researches in the following topics;

- Experimental investigation of the wear behavior using Addis Ababa light rail transit as a case study.
- Performance evaluation of the fatigue life of AALRT wheel/rail material; prediction and prevention.
- Optimization of the wheel/rail profile to reduce flange wear and surface fatigue.
- Developing a new fatigue resistance and wear resistance wheel/rail material for AALRT.
- FEM for Thermo-mechanical fatigue analysis of wheel/rail material in sliding and rolling motion.

References

[1] L. Wang, "Microstructure and Residual Stress State in the Contact Zone of Rails and Wheels," no. September, p. 166, 2002.

[2] H. Fontaine, J.-C. Belliard, M. G. Lambert, P. Javelot, Y. Stranger, and Artegrfica, *Un train en Afrique : Djibouti-Éthiopie = African train*. .

[3] F. M. Akello and L. U. Adoh, "Simulation of Power Generation from Vibration of Railway Track," vol. 9, no. 1, pp. 16–22, 2020.

[4] "Sub-Saharan Africa gets its first metro," *Econ.*, Sep. 2015.

[5] E. Nurse, "Sub-Saharan Africa gets its first metro," *CNN*, Nov. 2015.

[6] E. Sahle, "Ethiopia: Addis Light Rail Eases Transportation Problem," *AllAfrica*, Sep. 2015.

[7] A. Gebremichael, "Addis Ababa Institute Of Technology, Analysis of Rolling Contact Fatigue Damage and Fatigue Life Analysis of Rolling Contact Fatigue Damage and Fatigue Life," 2014.

[8] B. Sladojević, M. Jelić, and M. Puzić, "New requirements for the quality of steel rails," *Metalurgija-MJoM*, vol. 17, no. 4, pp. 213–219, 2011.

[9] B. Persson, F. Bucher, and B. Chiaia, "Elastic contact between randomly rough surfaces: Comparison of theory with numerical results," *Phys. Rev. B - PHYS REV B*, vol. 65, Apr. 2002.

[10] F. Bekele, "Effect Of Change Of Wheel-Rail Contact Geometry On Contact Fatigue Stresses," *Sch. Mech. Ind. Eng. Addis Ababa Inst. Technol.*, 2014.

[11] Aust, "Rail Defects Handbook RC 2400," no. A, p. 68, 2006.

[12] "Wear of Rails - Engineering Articles." [Online]. Available: http://www.engineeringarticles.org/wear-of-rails/. [Accessed: 12-Sep-2019].

[13] S. L. Grassie, "Rail corrugation: Characteristics, causes, and treatments," *Proc. Inst. Mech. Eng. Part F J. Rail Rapid Transit*, vol. 223, no. 6, pp. 581–596, 2009.

[14] "Rail Measurement- Longitudinal - Rail Engineering Services." [Online]. Available: http://railengineeringservices.co.uk/rail-measurement-longitudinal/. [Accessed: 02-Feb-2020].

[15] E. magel, M. Roney, J. Kalousek, and P. Sroba, "The blending of theory and practice in modern rail grinding," *Fatigue Fract. Eng. Mater. Struct.*, vol. 26, no. 10, pp. 921–929, Oct. 2003.

[16] O. Polach, "Characteristic parameters of nonlinear wheel/rail contact geometry," *Veh. Syst. Dyn.*, vol. 48, no. sup1, pp. 19–36, Dec. 2010.

[17] I. H. Ahmed, "fatigue analysis on welded rail joint using fem school of graduated studies postgraduate program in railway engineering, Fatigue Life Analysis on Welded Rail Joint using FEM," 2017.

[18] L. U. Adoh, M. F. Akello, N. Faraja, and P. Ishimwe, "Prevention of Railway Accident using Arduino Based Safety System : A case Study of Addis Ababa Light Rail Transit," vol. 8, no. 09, pp. 327–332, 2019.

[19] L. U. Adoh, M. Lovejoy, and A. fiona Mercy, "Safety Demonstration and Risk Management at Rail-Road Level Crossing at Addis Ababa Light Rail Transit Network,"

Int. J. Sci. Res. Sci. Eng. Technol., vol. 6, no. 5, pp. 103–109, 2019.

[20] A. Ekberg, "Rolling contact fatigue of railway wheels - A parametric study," *Wear*, vol. 211, pp. 280–288, Nov. 1997.

[21] W. J. Wang, W. Zhong, J. Guo, Q. Y. Liu, M. H. Zhu, and Z. R. Zhou, "Investigation on rolling contact fatigue and wear properties of railway rails," *Proc. Inst. Mech. Eng. Part J J. Eng. Tribol.*, vol. 223, no. 7, pp. 1033–1039, 2009.

[22] R. Enblom, "Simulation of Wheel and Rail Profile Evolution Wear Modelling and Validation," Jan. 2004.

[23] Z. Li, "Wheel-rail rolling contact and its application to wear simulation," Mar. 2002.

[24] B. Dirks, *Simulation and measurement of wheel on rail fatigue and wear*. 2015.

[25] U. Olofsson, Y. Zhu, S. Abbasi, R. Lewis, and S. Lewis, "Tribology of the wheel−rail contact – aspects of wear, particle emission and adhesion," *Veh. Syst. Dyn.*, vol. 51, pp. 1091–1120, Sep. 2013.

[26] R. Science, "Study on Numerical Analysis Method to Wheel / Rail Wear of Heavy Haul Train," pp. 837–846.

[27] R. Lewis *et al.*, "Mapping railway wheel material wear mechanisms and transitions," *Proc. Inst. Mech. Eng. Part F J. Rail Rapid Transit*, vol. 224, no. 3, pp. 125–137, 2010.

[28] M. Aquib Anis, J. P. Srivastava, N. R. Duhan, and P. K. Sarkar, "Rolling contact fatigue and wear in rail steels: An overview," *IOP Conf. Ser. Mater. Sci. Eng.*, vol. 377, no. 1, 2018.

[29] T. Kimura, M. Takemasa, and M. Honjo, "Development of SP3 rail with high wear

resistance and rolling contact fatigue resistance for heavy haul railways," *JFE Tech. Rep.*, vol. 16, no. 16, pp. 32–37, 2011.

[30] A. C. Athukorala, I. U. Wickramasinghe, and D. V. De Pellegrin, "Effect of different surface profile on wear of rail steel (AS1085.1) used in Australian heavy-haul railways," *Int. J. Mater. Eng. Innov.*, vol. 6, no. 4, pp. 225–242, 2015.

[31] S. Chang, Y. S. Pyun, and A. Amanov, "Wear enhancement of wheel-rail interaction by ultrasonic nanocrystalline surface modification technique," *Materials (Basel).*, vol. 10, no. 2, 2017.

[32] M. Schilke, *Degradation of Railway Rails from a Materials Point of View*, vol. Doctor of. 2013.

[33] H. Soleimani and M. Moavenian, "Tribological Aspects of Wheel–Rail Contact: A Review of Wear Mechanisms and Effective Factors on Rolling Contact Fatigue," *Urban Rail Transit*, vol. 3, no. 4, pp. 227–237, 2017.

[34] C. Franchima, "Broken Rail and Rail Heaters," 2017.

[35] "Trains from Brighton to London cancelled due to broken rail | The Argus." [Online]. Available: https://www.theargus.co.uk/news/16903457.trains-from-brighton-to-london-cancelled-due-to-broken-rail/. [Accessed: 02-Feb-2020].

[36] R. A. Smith, "Railways and materials: Synergetic progress," *Ironmak. Steelmak.*, vol. 35, no. 7, pp. 505–513, 2008.

[37] B. L. Singh and C. B. E. Sr, "Rolling Contact Fatigue in Rails – an Overview," vol. 209, pp. 1–15, 2008.

[38] D. Y. Jeong and O. Orringer, "Fatigue crack growth of surface cracks in the rail web," *Theor. Appl. Fract. Mech.*, vol. 12, no. 1, pp. 45–58, Oct. 1989.

[39] U. Olofsson and R. Nilsson, "Surface cracks and wear of rail: A full-scale test on a commuter train track," *Proc. Inst. Mech. Eng. Part F J. Rail Rapid Transit*, vol. 216, no. 4, pp. 249–264, Jul. 2002.

[40] N. Akeel, Z. Sajuri, and A. K. Ariffin, "Analysis of Rolling Contact Fatigue Damage Initiation At The Wheel-Rail Interface," *Aust. J. Basic Appl. Sci.*, vol. 5, Dec. 2011.

[41] T. N. Farris, L. M. Keer, and R. K. Steele, "Life Prediction for Unstable Shell Growth in Rails," *J. Manuf. Sci. Eng.*, vol. 112, no. 2, pp. 175–180, May 1990.

[42] J. Santamaria, E. G. Vadillo, and O. Oyarzabal, "Wheel–rail wear index prediction considering multiple contact patches," *Wear*, vol. 267, no. 5–8, pp. 1100–1104, 2009.

[43] J. Pombo, "Application of a computational tool to study the influence of worn wheels on railway vehicle dynamics," *J. Softw. Eng. Appl.*, vol. 5, no. 2, p. 51, 2012.

[44] h. Molatefi and z. Firouzabadi, "analyzing the interaction between wheel profile s1002 and iran rail profiles to investigate wheel-rail wear and wheelset behavior," *J. Transp. Eng.*, vol. 2, no. 4 (8), pp. 363–374, 2011.

[45] J. A. Williams, "Wear modelling: analytical, computational and mapping: a continuum mechanics approach," *Wear*, vol. 225–229, pp. 1–17, Apr. 1999.

[46] K. Kato and K. Adachi, "Wear Mechanisms 7.1 7.2," 2001.

[47] X. Jin and J. Zhang, "A complementary principle of elastic bodies of arbitrary geometry in rolling contact," *Comput. Struct.*, vol. 79, no. 29, pp. 2635–2644, 2001.

[48] R. B. Waterhouse, "Fretting wear," *Wear*, vol. 100, no. 1–3, pp. 107–118, Dec. 1984.

[49] J. F. Zheng, J. Luo, J. L. Mo, J. F. Peng, X. S. Jin, and M. H. Zhu, "Fretting wear behaviors of a railway axle steel," *Tribol. Int.*, vol. 43, no. 5–6, pp. 906–911, May 2010.

[50] A. Matsumoto *et al.*, "Creep force characteristics between rail and wheel on scaled model," *Wear*, vol. 253, no. 1–2, pp. 199–203, Jul. 2002.

[51] S. Zakharov, I. Komarovsky, and I. Zharov, "Wheel flange/rail head wear simulation," *Wear*, vol. 215, no. 1–2, pp. 18–24, 1998.

[52] C. C. Viáfara, M. I. Castro, J. Vélez, and A. Toro, "Unlubricated sliding wear of pearlitic and bainitic steels," *Wear*, vol. 259, pp. 405–411, Jul. 2005.

[53] R. Lewis, R. Dwyer-Joyce, U. Olofsson, and R. I. Hallam, *Wheel material wear mechanisms and transitions*. 2004.

[54] Windarta, "Application pin-on-disc method for wear rate prediction on interaction between rail and wheel," *IOP Conf. Ser. Mater. Sci. Eng.*, vol. 403, no. 1, pp. 0–6, 2018.

[55] M. A. Gökçe and O. Ç. Nuri, "Inspection of friction and wear properties of railway rails," vol. 16, no. 2, pp. 89–95, 2013.

[56] J. F. Archard, "Contact and Rubbing of Flat Surfaces," *J. Appl. Phys.*, vol. 24, no. 8, pp. 981–988, Aug. 1953.

[57] J. Lengiewicz and S. Stupkiewicz, "Efficient model of evolution of wear in quasi-steady-state sliding contacts," *Wear*, vol. 303, no. 1–2, pp. 611–621, 2013.

[58] N. Robinson, *North, East and Central Africa*. Barnsley, UK: World Rail Atlas, 2009.

[59] A. G. Evans and D. B. Marshall, "WEAR MECHANISMS IN CERAMICS.," 1981, pp. 439–452.

[60] H. C. Meng and K. C. Ludema, "Wear models and predictive equations: their form and content," *Wear*, vol. 181–183, no. PART 2, pp. 443–457, 1995.

[61] T. Mishra, M. de Rooij, M. Shisode, J. Hazrati, and D. J. Schipper, "A material point method based ploughing model to study the effect of asperity geometry on the ploughing behaviour of an elliptical asperity," *Tribol. Int.*, vol. 142, 2020.

[62] K. B. Rathod and D. I. Lalwani, "Modeling of flank wear progression for coated cubic boron nitride tool during hard turning of AISI H11steel," *Mater. Today Proc.*, vol. 5, no. 2, pp. 6692–6701, 2018.

[63] M. Pau, F. Aymerich, and F. Ginesu, "Distribution of contact pressure in wheel-rail contact area," *Wear*, vol. 253, no. 1–2, pp. 265–274, 2002.

[64] A. Meghoe, R. Loendersloot, and T. Tinga, "Rail wear and remaining life prediction using meta-models," *Int. J. Rail Transp.*, vol. 00, no. 00, pp. 1–26, 2019.

[65] R. G. Bayer and R. G. Bayer, *Mechanical wear prediction and prevention*. M. Dekker New York, 1994.

[66] S. Bahadur, "Wear Research and Development," *J. Lubr. Technol.*, vol. 100, no. 4, pp. 449–454, Oct. 1978.

[67] T. F. J. Quinn, "Oxidational wear," *Wear*, vol. 18, no. 5, pp. 413–419, 1971.

[68] H. Arabnejad, A. Mansouri, S. A. Shirazi, and B. S. McLaury, "Abrasion erosion modeling in particulate flow," *Wear*, vol. 376–377, pp. 1194–1199, 2017.

[69] H. C. Meng and K. C. Ludema, "Wear models and predictive equations: their form and content," *Wear*, vol. 181–183, pp. 443–457, Mar. 1995.

[70] J. R. Barber, "Is modeling in tribology a useful activity?," in *Tribological Modeling for Mechanical Designers*, ASTM International, 1991.

[71] S. K. Rhee, "Wear equation for polymers sliding against metal surfaces," *Wear*, vol. 16, no. 6, pp. 431–445, 1970.

[72] F. T. Barwell, "The contribution of particle analysis to the study of wear of metals," *Wear*, vol. 90, no. 1, pp. 167–181, 1983.

[73] J. F. Archard, "Contact and rubbing of flat surfaces," *J. Appl. Phys.*, vol. 24, no. 8, pp. 981–988, 1953.

[74] M. S. Sichani, R. Enblom, and M. Berg, *Non-Elliptic Wheel-Rail Contact Modelling in Vehicle Dynamics Simulation*, vol. 3, no. 3. 2014.

[75] G. W. Stachowiak and A. W. Batchelor, "Engineering Tribology, Chap. 13, publ." Butterworth Heinemann, 2006.

[76] A. Y. Suh, A. A. Polycarpou, and T. F. Conry, "Detailed surface roughness characterization of engineering surfaces undergoing tribological testing leading to scuffing," *Wear*, vol. 255, no. 1–6, pp. 556–568, 2003.

[77] H. Aziz Ameen, K. Salman Hassan, and E. Mohamed Mhdi Mubarak, "AMERICAN JOURNAL OF SCIENTIFIC AND INDUSTRIAL RESEARCH Effect of loads, sliding speeds and times on the wear rate for different materials," no. 1, pp. 99–106, 2011.

[78] K. Kato and K. Adachi, "Friction and wear of passive metals and coating," 2001, p. 10.

[79] G. Kosuri, "M ASTE R ' S THE SI S Rolling / sliding wear resistance of steels with different microstructures," 2010.

[80] J. G. Alotaibi, B. F. Yousif, and T. F. Yusaf, "Wear behaviour and mechanism of different metals sliding against stainless steel counterface," *Proc. Inst. Mech. Eng. Part J J. Eng. Tribol.*, vol. 228, no. 6, pp. 692–704, 2014.

[81] B. S. Windarta, M., "Influences of Applied Load.Pdf," *Journal of Applied Sciences*, vol. 11, no. 9. pp. 1636–1641, 2011.

[82] S. Iwnicki, M. Spiryagin, C. Cole, and T. McSweeney, *Handbook of railway vehicle dynamics*. CRC press, 2019.

Appendixes

Appendix A

Specific wear rate of rail material with different friction coefficient and speed.

Wheel Load of 51392.33 N and speed of 20 Km/h			**Wheel Load of 51392.33 N and speed of 35 Km/h**			**Wheel Load of 51392.33 N and speed of 70 Km/h**		
COF	Wear Rate X 10^{-6}	Max contact pressure	COF	Wear Rate X 10^{-6}	Max contact pressure	COF	Wear Rate X 10^{-6}	Max contact pressure
0.1	0.000453	519.39	0.1	0.00251	519.51	0.1	0.05929	570.3
0.2	0.003151	492.74	0.2	0.049237	581.9	0.2	0.194	655.3
0.3	0.004917	502.73	0.3	0.091624	600.5	0.3	0.529278	868.4
0.4	0.071597	464.12	0.4	0.397207	391.7	0.4	1.11084	713.8
0.5	0.09054	501.45	0.5	0.554903	312.2	0.5	1.271234	758
Wheel Load of 48428.7 N and speed of 20 Km/h			**Wheel Load of 48428.7 N and speed of 35 Km/h**			**Wheel Load of 48428.7 N and speed of 70 Km/h**		
COF	Wear Rate X 10^{-6}	Max contact pressure	COF	Wear Rate X 10^{-6}	Max contact pressure	COF	Wear Rate X 10^{-6}	Max contact pressure
0.1	0.000354	612.89	0.1	0.00150	612.9	0.1	0.0257	612.89
0.2	0.0026	612.86	0.2	**0.029168**	612.87	0.2	0.1006	612.857
0.3	0.0041	612.85	0.3	**0.0575**	612.85	0.3	0.3243	612.85
0.4	0.061	612.847	0.4	**0.3194**	612.847	0.4	1.022	612.847
0.5	0.087	612.845	0.5	**0.4845**	612.846	0.5	1.1945	612.846
Wheel Load of 35970 N and speed of 20 Km/h			**Wheel Load of 35970 N and speed of 35 Km/h**			**Wheel Load of 35970 N and speed of 70 Km/h**		
COF	Wear Rate X 10^{-6}	Max contact pressure	COF	Wear Rate X 10^{-6}	Max contact pressure	COF	Wear Rate X 10^{-6}	Max contact pressure
0.1	0.000247	612	0.1	**0.00982**	612.89	0.1	0.0168	612.89
0.2	0.00081	613	0.2	**0.019507**	612.849	0.2	0.09776	612.849
0.3	0.0029	612.841	0.3	**0.02917**	612.841	0.3	0.235	612.841
0.4	0.0046	612.838	0.4	**0.2941**	612.838	0.4	0.799	612.838
0.5	0.0569	612.837	0.5	**0.4339**	612.837	0.5	0.9373	612.837

Appendix B

Hertz Coefficients for $A/B<1$ [82]

θ(deg)	M	N	θ(deg)	M	N	θ(deg)	M	n
0.5	61.4	0.1018	10	6.6	0.311	60	1.49	0.72
1	36.89	0.1314	20	3.81	0.413	65	1.38	0.76
1.5	27.48	0.1522	30	2.73	0.493	70	1.28	0.8
2	22.26	0.1691	35	2.4	0.53	75	1.2	0.85
3	16.5	0.1964	40	2.14	0.567	80	1.13	0.89
4	13.31	0.2188	45	1.93	0.604	85	1.06	0.91
6	9.79	0.2552	50	1.75	0.641	90	1	1
8	7.86	0.285	55	1.63	0/678			

Appendix C

Volumetric loss for Overload capacity of the train

Coefficient of friction	Sliding dist = 111.2 m	Sliding dist = 194.44 m	Sliding dist = 388.9 m
S/N	**volumetric loss X 10^{-8} (mm^3)**	**volumetric loss X 10^{-8} (mm^3)**	**volumetric loss X 10^{-8} (mm^3)**
0.1	0.00980745	0.0950035	6.7329724
0.2	0.06821915	1.48512045	22.03064
0.3	0.10645305	1.95542184	60.10480968
0.4	1.55007505	26.38928495	126.1469904
0.5	1.960191	32.35807855	144.361333

Volumetric loss for Seating capacity of the train

Coefficient of friction	Sliding dist = 111.2 m	Sliding dist = 194.44 m	Sliding dist = 388.9 m
S/N	**volumetric loss X 10^{-8} (mm^3)**	**volumetric loss X 10^{-8} (mm^3)**	**volumetric loss X 10^{-8} (mm^3)**
0.1	0.007221246	0.0567153	1.833438
0.2	0.0530374	1.1300256	7.176804
0.3	0.0836359	0.7134	23.135562
0.4	1.244339	15.6948	72.90948
0.5	1.774713	24.416115	85.21563

Volumetric loss for Empty capacity of the train

Coefficient of friction	Sliding dist = 111.2 m	Sliding dist = 194.44 m	Sliding dist = 388.9 m
S/N	volumetric loss X 10^{-8} (mm^3)	volumetric loss X 10^{-8} (mm^3)	volumetric loss X 10^{-8} (mm^3)
0.1	0.003742297	0.0317844	0.890232
0.2	0.01227231	0.66402909	5.1803024
0.3	0.0439379	0.50775579	12.45265
0.4	0.0696946	10.4385267	42.33901
0.5	0.8620919	14.276493	49.667527